MECHATRONIC DESIGN AND ANALYSIS OF A SOLENOID BASED INJECTOR

A Thesis

by

Ayhan Yağcı

Submitted to the
Graduate School of Sciences and Engineering
In Partial Fulfillment of the Requirements for
the Degree of

Master Science

in the
Department of Mechanical Engineering

Özyeğin University
August 2019

MECHATRONIC DESIGN AND ANALYSIS OF A SOLENOID BASED INJECTOR

Approved by:

Asst. Prof. Dr. Özkan Bebek, Advisor
Department of Mechanical Engineering
Özyeğin University

Asst. Prof. Dr. Altuğ Başol
Department of Mechanical Engineering
Özyeğin University

Assoc. Prof. Dr. Güllü Kızıltaş Şendur
Faculty of Engineering and Natural Sciences
Sabanci University

Date Approved: 19 August 2019

To my family

ABSTRACT

Injectors are devices for producing spray, namely, for creating small liquid droplets. In the automotive industry, generally, the injectors are used to inject fuel into the combustion chamber. In recent years, systems are developed to clean the exhaust gases produced by the diesel engines. In these systems, injectors are also used to reduce the NOx emissions, which are harmful to the environment, by spraying urea solution to the exhaust gas.

Injectors are compact systems with parts like atomizer, actuator, plunger, spring, needle, and seat. The design process of each component is separate, but they must be designed together. Once assembled, replacing parts of the system can be quite challenging. The aim of this thesis is to design a modular solenoid-actuated injector mechanism so that tests with a variety of subsystem components could be conducted.

In this thesis, the working principles of solenoid actuators used in injectors have been studied. An injector mechanism which is modular in all parts has been designed, produced and tested. The components of this modular design can be changed independently, and the efficiency of the updated system can be investigated. This mechanism has shortened the injector development and testing process. The prototype was tested in demanding conditions similar to commercial injectors and successfully opened in 1.2 milliseconds at 80-micrometer displacement under 5 bars liquid pressure.

ÖZETÇE

Enjektörler, küçük sıvı damlacıkları oluşturmak için kullanılan cihazlardır. Otomotiv endüstrisinde, genel olarak enjektörler yanma odasına yakıt püskürtmek için kullanılır. Son yıllarda, dizel motorlarının ürettiği egzoz gazlarını temizlemek için, bazı sistemler geliştirilmiştir. Bu sistemlerde, enjektörler ayrıca çevreye zararlı olan NOx emisyonlarını azaltmak amacıyla egzoz gazına üre çözeltisi püskürtmek için de kullanılmaktadır.

Enjektörler; atomizer, aktüatör, piston, yay, iğne ve oturak gibi parçalara sahip kompakt sistemlerdir. Her bir bileşenin tasarım süreci ayrıdır, ancak birlikte tasarlanmaları gerekir. Tüm enjektör bir kez monte edildiğinde, sistemin parçalarını değiştirmek oldukça zor olabilir. Bu tezin amacı, modüler olarak enjektör mekanizması tasarlamaktır, böylece her bir parçanın farklı modelleri ile testleri yapılabilir.

Bu tez çalışmasında, enjektörlerde kullanılan solenoid aktüatörlerin çalışma prensipleri incelenmiştir. Tüm parçaları modüler olan bir enjektör mekanizması tasarlanmış, üretilmiş ve test edilmiştir. Bu modüler tasarımın bileşenleri, bağımsız olarak değiştirilebilir ve güncellenmiş sistemin verimliliği araştırılabilir. Bu mekanizma, enjektör geliştirme ve test sürecini kısaltmaktadır. Prototip, ticari enjektörlere benzer zorlu koşullarda test edildi ve enjektör iğnesini 1.2 milisaniyede, 5 bar sıvı basıncı altında, 80 mikrometre yer değiştirerek başarıyla açıldı.

ACKNOWLEDGEMENTS

My deepest recognition goes to my supervisor, Professor Özkan Bebek for his unconditional help, excellent knowledge of the field and providing the whole team with an excellent atmosphere for doing research. I am very grateful for his guidance and support during my master study. There are no words to express my gratitude for all of the help and support he offered to me during my studies. I am thankful for his encouragement, help, and patience which enabled me to complete this thesis.

I would also like to thank Professor Özgür Ertunç for his support and sharing his knowledge which helped me improve my research throughout my master's education.

My thanks also go to the other members of the thesis defense committee, Professor Altuğ Melik Başol and Professor Güllü Kızıltaş Şendur. I am so glad to see them in my thesis defense committee.

I also want to thank all the members of the Özyeğin Robotics Lab members and Fluid Dynamics and Spray Laboratory members for their friendship. We worked together nights and days and shared lots of good times in the Robotics Lab.

Special thanks go to my family with my deepest gratitude. They supported me to complete my thesis from every angle. They made a lot of sacrifices during my educational life. I am so grateful for everything.

This research was done at the Robotics Laboratory and Fluid Dynamics and Spray Laboratory at Özyeğin University; supported by the the Scientific and Technological Research Council of Turkey (TÜBİTAK), grant number 115M093.

TABLE OF CONTENTS

LIST OF TABLES

LIST OF FIGURES

CHAPTER I

INTRODUCTION

Solenoids are found in a variety of sizes, configuration and load requirements as the use of electronic fluid control systems increase to replace conventional hydraulics and mechanical systems. Solenoid valves can be used for a wide array of industrial applications, including general on-off control, calibration and test stands, pilot plant control loops, process control systems, and various original equipment manufacturer applications. They are utilized especially in automotive applications such as fuel injection, exhaust gas recirculation (EGR), transmission control, speed-sensitive steering system, airbag deployment, etc. [1].

In the automotive industry, injectors are used for spraying fuel into the combustion chamber of the engine, for spraying urea over the exhaust gas in the after-treatment system, and for injecting fuel over to the diesel particle filter.

This thesis aims to design the mechatronic components of a solenoid based urea injector for diesel engines. Diesel exhaust fluid is a homogenized solution of water and urea which is commercially sold and used in Selective Catalytic Reduction (SCR) systems to control the emission of a diesel engine. SCR is an advanced post-combustion NOx control system which converts NOx rich exhaust stream of a diesel engine to less hazardous nitrogen (N_2) and water vapor (H_2O) by series of chemical reduction. Since 2014, most diesel cars that meet the Euro 6 standard, ie NOx output below 0.08 g/km, will be equipped with an SCR system. This is reduced by 97 percent up to Euro 6, considering the Euro 0 requirements, where there are no standards [2].

There are two important criteria to measure an injector's spray outcome. The first is the quantity and the second is quality. The atomizer (nozzle) affects the quality of

the spray. Quality refers to the diameter of the droplets, the spray dispersion angle and the spray penetration. Since atomization is a broad research field, related studies are not discussed in this thesis; tests were performed using off-the-shelf atomizers. The quantity on the other hand mainly depends on the actuator selection and the mechanical design of the injector, which is the main focus of this thesis.

Figure 1 shows the cross-section of the inner workings of a fuel injector. In an injector, a solenoid actuator regulates the amount of spray. The solenoid actuator generates the force to lift the armature when the coil is energized. When this force is higher than the spring force, the armature moves towards the coil, causing the steel ball to stay out of the seat. Thus, the liquid escapes from the nozzle. This creates spray. In general, the solenoids are custom designed for each application. Design for injectors would require solenoids to have minimum motion time, long service life, and low cost. As it is seen, the system has a compact design and these subsystems need to be designed and tested again and again especially during the research and development phase. Therefore, a modular injector mechanism is needed to improve the design and testing process of the injectors. Thus, each subsystem which are the nozzle, the solenoid actuator, and the spring, can be designed and produced repeatedly and tested on the same platform.

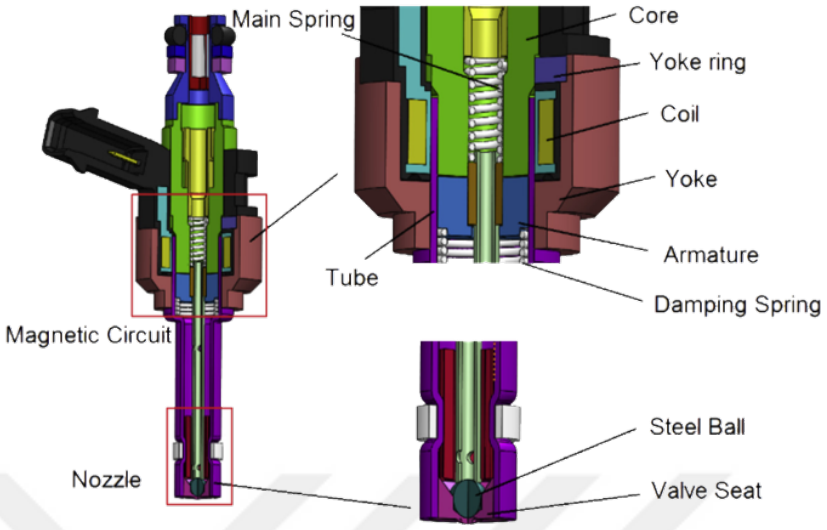

Figure 1: Cross section of a fuel injector [3]. Magnetic circuit refers to solenoid actuator. The atomizer and the tip of the needle are shown as the nozzle.

1.1 Thesis Contribution

This work has led several contributions in designing an injector system for research and development.

First, the working principles of solenoid actuators were investigated with a large solenoid actuator that has relatively slow motion. The effects of the parameters that are important for motion were studied. At the same time, the motion of the solenoid actuator was analyzed using finite element software and the dynamic behavior of the parametric designs were modeled according to the changing materials and these analyses were verified with experiments. This part of the study was presented at AIAC-2017 [4].

In the second part of the thesis, injector mechanisms in the literature were studied. The operating systems of the injectors were examined and the physics behind magnetic, electrical, mechanical fluid and thermal subsystems were reviewed. Also, the injector parts affecting the control of the physical system was described. Analyses

were performed to find out the forces generated by solenoid actuators with varying displacement distances and varying current characteristics. Then these analyzes were validated with experiments. The ISEF 2019 article [5] explains how to design a modular injector mechanism with many subsystems to be used in research and development.

1.2 Thesis Outline

This thesis consists of seven chapters. It is organized as follows. In this chapter, the injector mechanism is introduced and approached problem is explained. In the second chapter, the literature about solenoid actuators and injector mechanisms is summarized. The design parameters and dynamic characteristics of the solenoid actuators were investigated in Chapter 3. The types of injectors and the scientific modeling of the injector mechanism are explained in Chapter 4. The design and manufacturing process of the prototype injector and the problems encountered at this stage are presented in Chapter 5. In Chapter 6, the use of the injector as well as the analysis and testing of the prototype injector and its subsystems are described. Finally, the conclusion is given in Chapter 7.

CHAPTER II

RELATED WORKS IN THE LITERATURE

In this thesis, solenoid actuators and injector mechanisms in the literature are reviewed. For an injector to perform accurate dosing, the actuator must work accurately. The literature search focuses on two topics. The first is the investigation of solenoid actuation, and the second is the use of solenoid actuators for injection mechanisms.

2.1 Solenoid Actuator

In literature, there are many studies conducted about the solenoid systems. The following summarizes the work related to solenoid actuator design, analysis, and optimization.

The dynamic characteristics of the solenoid determine how fast the actuator will open and close in applications [6]. For example, in an fuel injector, the duration of motion of a solenoid actuator to be used for atomization determines the amount of spray, which is crucial to maintain fuel economy [7].

It is possible to examine the solenoid by dividing it into three subsystems, which are magnetic, electrical and mechanical. The combined behavior of these subsystems determine the solenoid's overall dynamic response. There are some design recommendations for solenoids that have the minimum closing time. These recommendations are to keep the magnetic force at the maximum value while minimizing the current [8]. These refer to variables in the most subsystems that act to reduce the closing time and increase the magnetic force [9].

The electrical subsystem represents the coil, which can be modelled as a series combination of resistor and inductor element. The voltage applied to the terminal

of the solenoid coil generates current as a function of time. The magnetic force to be generated is directly proportional to the instantaneous current of the coil. Low resistance of solenoid causes high current flow when constant voltage is applied. But, high current flow creates Joule heating, which causes permanent mechanical damage to the solenoids' parts [10]. In order to avoid this problem, it is necessary to run the solenoid using an appropriate drive strategy. It is possible to achieve the same dynamic characteristics with different driving strategies and optimize temperature values [3].

The forces acting on the moving part of solenoid are magnetic force applied on plunger, the force of spring, gravitational force, friction force and possible external forces such as the pressure acting on the plunger. All these forces are components of the mechanical subsystem. Magnetic force occurs as a result of magnetic and electric subsystems. The gravitational force is related to the mass of the moving parts. Frictional force can be neglected because different solutions have been developed to prevent friction on surfaces in solenoid systems. The easiest to change from mechanical forces is the spring force. The literature [11, 12] shows the variation of dynamic characteristics according to different springs. Also, the mass of the plunger can be changed according to design. [13].

The magnetic subsystem of solenoid consists of a magnetic circuit which is comprised of at least one closed path containing a magnetic flux. When the current is passed through the coil, a magnetic flux appears in the air gap and pulls or pushes the piston to close the air gap. When designing the magnetic circuit of the solenoid, shapes and materials of components must be considered. Design limitations are the shapes of solenoid components and air gaps, but they are connected to each other. When the magnetic model is prepared, the air gaps which are in the magnetic circuit have a negative effect on the magnetic force. Some studies in the literature [14–16] have reduced the air gap and optimizing the shape of the solenoid parts. Also new

models that work faster and stronger were obtained. Other parameter of magnetic circuit is material of solenoid actuator. The ferrous material of all parts in magnetic cycle are modeled with nonlinear B-H (flux density vs. field intensity) curves to capture important saturation effect in solenoid that could limit the force and motion. Previously, the plunger was tested with different materials such as permanent magnet and soft magnetic material to determine their dynamic characteristics [17]. In literature, different analyzes were made with a limited number(maximum 3 or 4) of materials and their results were compared [4, 18].

Commonly magnetic properties of magnetic materials are describing by hysteresis loop where the measured magnetic flux density is entered above the given magnetic field intensity. First, it starts at the zero point of the scales where the material is not magnetized. An increasing magnetic field intensity applies non-linearly increasing a magnetic flux density to the material up to a point of saturation, where a further increased magnetic field intensity does not raise the magnetic flux density anymore. The shape is called the initial magnetization curve. Magnetic flux density can be seen as the magnitude of the magnetic force applied to magnetic materials in the magnetic field. Solenoid actuators usually use magnetic steels. According to the in magnetic types, steels can be divided into non-magnetic, hard magnetic and soft magnetic. Materials that are not affected in any way by the magnetic field can be called non-magnetic, materials like aluminum and copper. Hard magnetic materials are those that constantly producing a magnetic field and they are also known as a permanent magnets. Soft magnetic materials are those that can be magnetized quickly when they enter magnetic field.

Based on electromagnetic computations magnetic, electrical and mechanical behavior of the solenoid were obtained using Finite Element Analysis via ANSYS-Electronics [19]. ANSYS-Electronics uses energy conservation as the finite element method (FEM) [20]. It is not only the magnetic force characteristics and the mass

of the moving part that determine the opening behavior, but also the value of magnetic force depends on the shape of the solenoid parts, the current of the coil and magnetic permeability of various soft magnetic material components. To study the dynamic characteristics of the solenoid in detail, a simulation analysis of its dynamic performance is an effective method. The finite element model predictions are used to determine the dynamic characteristic. From these analyses, operating behavior of the solenoid could be predicted. A simulation model of the solenoid that has high accuracy is thus indispensable. Its accuracy could be checked by experiments. Different materials could be used in the analyzes. It is known that the motion time of the plunger depends on the magnetization time of the material [21].

2.2 Working Principles of Injector Mechanisms

Injector is a pump and valve mechanism, that sprays liquid intermittently to intended volume. An injector has many core elements, relating to at least five physical fields of science including mechanical, electrical, magnetic, thermal and fluid dynamics [22]. All the subsystems must work accurately to achieve the desired spray performance. An injector starts spraying when the solenoid actuator is triggered by supply voltage and consequently the spray is stopped by recoil force created by a spring after the applied voltage of the solenoid actuator is cut. The fundamental challenges for a successful injection is the quantity and the quality of the spray [23]. Quality of the spray depends on the atomizer of the injector [24], whereas the accurate spray amount is related to the speed of the solenoid actuator. Many studies have been conducted on solenoid actuators to adjust the sprayed fluid amount [22], [25].

Although solenoid actuator driven injectors are widely used and applied to various applications in automotive industry [26], indirect acting piezoelectric injectors represent a valid alternative [27]. However, due to lower manufacturing costs of solenoid injectors over the piezoelectric injectors, solenoid technology should be the preferred

option when indirect acting injectors are considered [28].

It is challenging to manufacture a compact injector especially for research and development because special manufacturing methods and high tolerances are required [29]. A test injector system with exchangeable atomizers, springs and solenoid actuators would benefit the researchers during initial development phase [30] . Injectors having a better dynamic response could be designed with the help of FEM [6]. Electro-magneto-mechanical system is one of the key components to be studied in the beginning phase of the design [16], [30].

Injector structures in the literature are examined and shown in Figures 2, 3, 4, 5 and 6. Since most of the injectors' design criteria are trade secrets, many parameters are hidden in the critical design point, even in academic sources. However, it is understood from these publications that low resistance-bobbins are preferred. Because the smaller the resistance, the greater the current draw slope of the coil, the faster the movement of the actuator. Another feature is that the displacement of the plunger or injector needles is generally kept below 1 mm to provide fast response.

Hung's injector [31] has 0.9 mm plunger displacement which is highest displacement in reviewed literature, and injector's plunger mass is 8 g. Coil is operated at 12 volts and its resistance is 1.6 Ohms. Winding number of the coil is 272. The spring coefficient is 2290 N/m. The cross-sectional image is shown in the Figure 2.

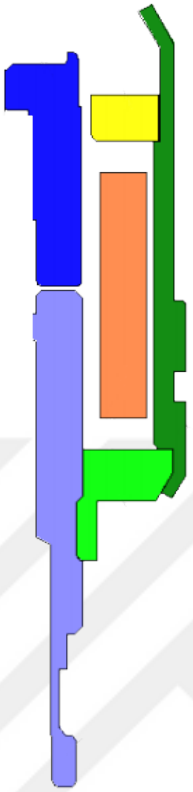

Figure 2: Cross section of Hung's injector with many design parameters known [31] (272 turns, 12 Volt, 1.6 ohm, 2290 N/m spring coefficient, 8 gram plunger, 0.9 mm displacement).

Subic's injector [13] has comparable 3 distinct designs. Plunger displacements are 2.47, 3 and 5 mm, whose masses vary between 0.4 and 0.75 g. Turning number of coils are 4679, 4800 and 7035. 430-grade stainless steel and cold rolled steel were used as magnetic materiala. Coils were applied 12 volts. In [13], the electrical, magnetic and mechanical models of the solenoid actuators used in the injector were explained. The cross-sectional view of what is shown in Figure 3.

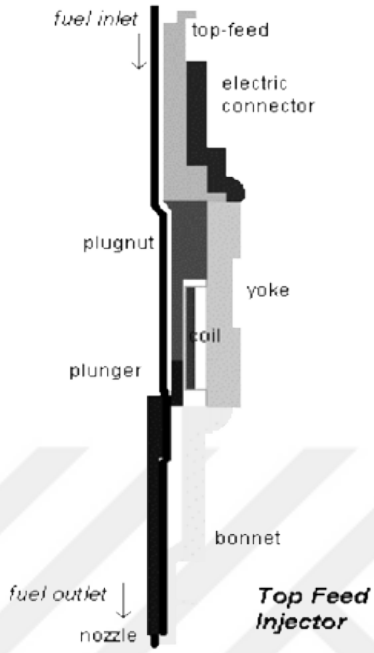

Figure 3: Cross section of Subic's injector [13] with finite element analysis model explained. (12 volt, 0.4-0.7 g. needle mass, 2.47-5 mm displacement, materials are cold rolled and 430 steel, 4679-7035 turning number)

Lee [32] compared 2 different needle designs. The difference between the designs is the way that liquid reaches the atomizer. In one, the fluid is carried around the needle, while in the other, the liquid comes out of the needle. This variation also changes the force of the fluid applied to the injector needle, thus changing the dynamic movement. The displacement amount of this injector needle is 0.3 mm. The cross-sectional view of what is shown in Figure 4.

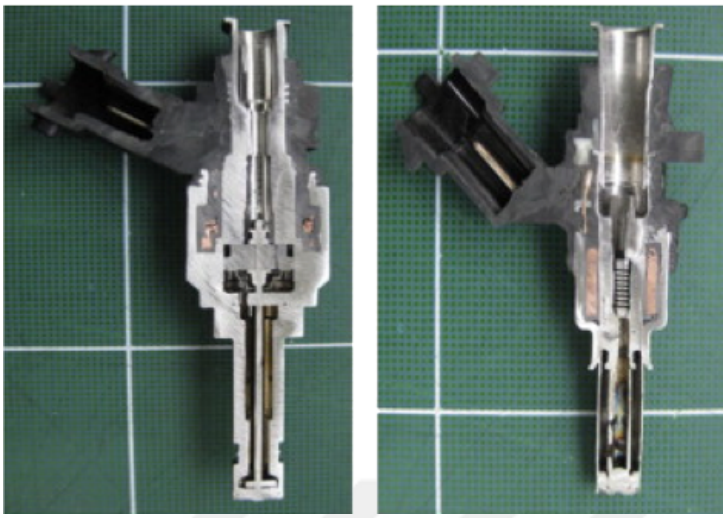

Figure 4: Cross section of Lee's injector [32] studied on injector needle.

Hong's injector [31] has 0.6 mm plunger displacement whose mass varies between 9 and 16 g. It can produce a maximum force of 155 N. The opening time of the injector is specified to be 1.5 milliseconds. The cross-sectional view is shown in Figure 5.

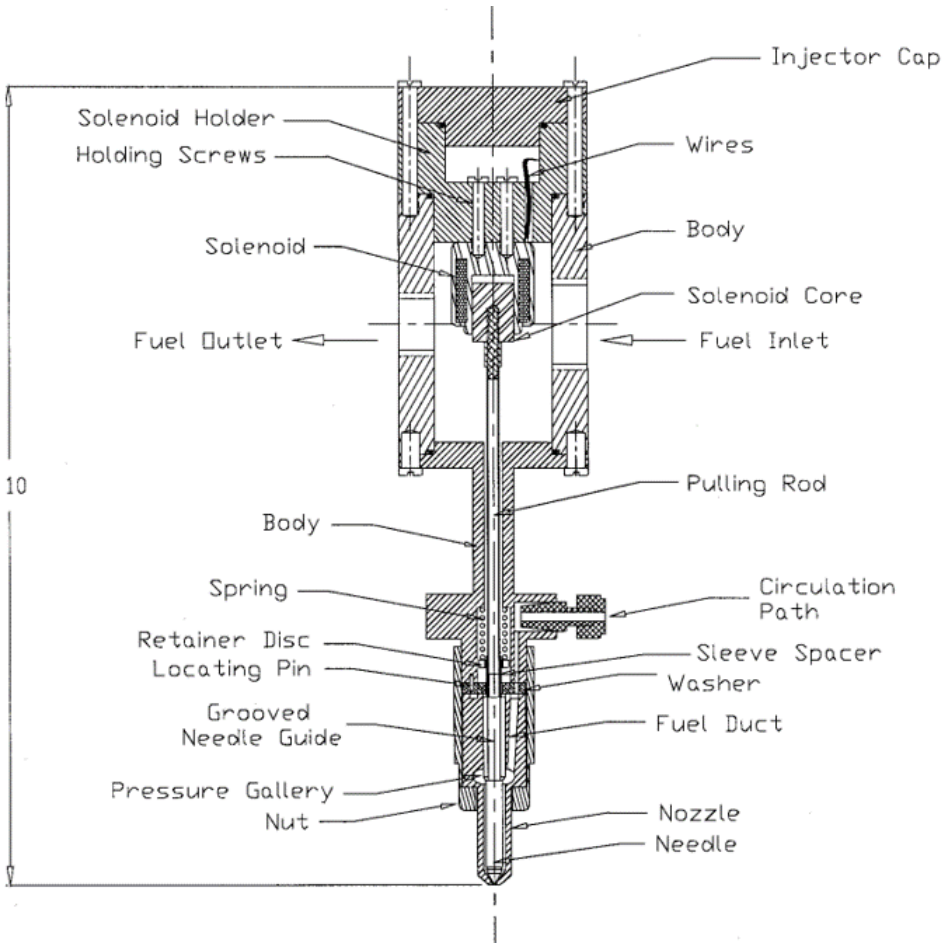

Figure 5: Cross section of Hong's injector [33] capable of generating 155 N. (9-16 gr plunger mass, 155 N max force, opening time 1.5 ms, displacement 0.6 mm)

Chowdhury's injector [34] injects CNG (Compressed natural gas). It has a 50-micron stroke length. It has 678 windings using 0.65 mm diameter copper wire. In this injector the liquid is collected in a pool away from the coil, not through the coil. Although it has a coil, the operating system is different from the solenoid actuators. This type of injectors uses a special magnetic material which is magnetostrictive (Terfenol-D). The magnetostrictive materials expand and contract in the magnetic field, allowing movement of the needle within the injector. The cross-sectional view is shown in Figure 6.

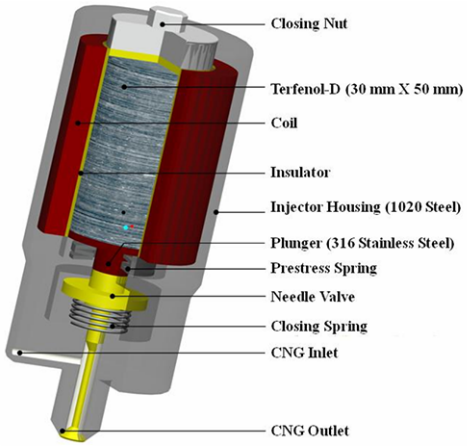

Figure 6: Cross section of Chowdhury's injector [34] collecting fluid in a pool. 0.05 mm displacement, 678 turns in 8 layers, 0,65 mm diameter copper wire, 5 mm coil thickness and housing material is 1020 steel.

As a result of these investigations, it is concluded that an injector has two important outputs. The first of these is the geometry of the hole where the droplets leave the injector, and the second is the actuator part which enables the injector to open and close. Variables such as coil parameters, displacement distance and plunger travel time have always provided ideas for an actuator design.

2.3 Design Requirements

Within the scope of this thesis, the structural part that will hold the actuator and the atomizer together is to be designed and manufactured. For this purpose, a modular design is preferred so that different actuators with different atomizers could be tested. This way, the need to built many injector prototypes is eliminated.

Given these design criteria, first of all, the main parts of the injector should be modular. If the subsystems of the injector mechanism to be used in research and development stages are designed and manufactured independently, many combinations of subsystems can be tested on this single platform.

For proper operation of the injector system, it is important to control the fluid flow

in the injector. For this reason, undesired leakages should be prevented by making the correct sealing while the injector is running.

As in the literature, the actuator of the injector must have a displacement of less than 1 mm and the travel time should be less than 2 milliseconds. An injector of this capacity can provide the correct dosing and be used in the industry. The design specifications for the injector is given in Table 1.

Table 1: Design Requirements of Solenoid Based Prototype Injector

Item		**Value**	**Unit**
Size Constraints	Length	<200	mm
	Width	<100	mm
	Depth	<100	mm
Fluid	Internal Pressure	2 - 6	bars
	Leak-proof	-	-
Motion	Opening time	<2	ms
	Needle displacement	0.05-0.6	mm
Solenoid Actuator	Coil Current	<3	A
	Coil Voltage	24	V
Material Constraints	Parts in contact with liquid	Stainless steel	-
	Others	High strength steel	-

CHAPTER III

SOLENOID ACTUATOR DESIGN

The solenoid actuator is one of the most important parts of the injector dosing mechanism. The solenoid actuator needs to be well understood to complete the electromechanical design of the injector. Solenoid actuators have a multi-physical phenomenon consisting of magnetic, electrical and mechanical sub-systems. The movement of the solenoid actuators used in the injector has a very short period of motion time (less than 2 milliseconds) and a very small displacement (less than 0.4 mm) [25]. It is quite difficult to perform analysis and experiments in this limited region due to the small physical quantities. Therefore, to better understand the phenomenon of the solenoid actuator, analysis and testing steps were carried out on a larger solenoid actuator.

In this research, the plunger-type solenoid actuator was chosen. Because this type of configuration has a single main air gap for flux to cross and one parasitic air gap that is perpendicular to the main (case) part. Since the piston type solenoid actuators have only one main air gap and this air gap is perpendicular to the magnetic cycle, this leakage does not cause interference even if there is leakage in the magnetic flux [35]. The plunger-type is more suitable for fast-moving applications and small stoke such as an injector and other fast-acting solenoid actuators.

Solenoid actuator was modeled using computer-aided design (CAD) software. The CAD of the solenoid actuator is shown in Figure 7. The coil is formed by winding the insulated copper wire around the coil holder which is a kind of plastic material. The coil is the source of the electromagnetic force. The plunger is the moving part that moves by the effect of electromagnetic force. The case holds all parts together. The air gap determines the distance the plunger can move.

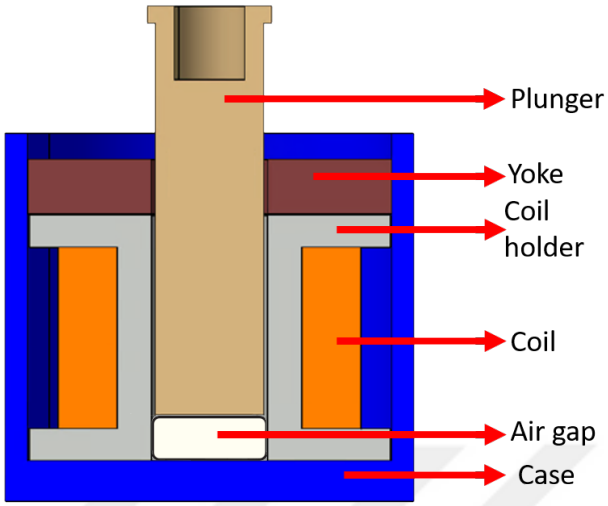

Figure 7: Cross section of solenoid actuator model

3.1 Modeling Solenoid Actuator

It is necessary to identify the relationships between the design parameters of the solenoid actuator and their effects on solenoid's performance. These relationships are shown in Figure 8. The output of one subsystem creates the input of the other subsystem. For example, current, which is an output of the electrical subsystem, is the input of the magnetic subsystem. Furthermore, the magnetic force, which is an output of the magnetic subsystem, is the input of the mechanical subsystem. In the solenoid actuator system, the voltage must be defined as an input to acquire the motion. When the voltage to the coil is applied, it creates a time-varying current depending on the coil resistance and inductance. The input of the magnetic subsystem is the current. The current producing the magnetic force highly depends on the magnetic properties of the material used and the shape and position of the materials. Thus, the variety and magnetic efficiency of the metals that can be selected for the solenoid actuator is increased. The mechanical subsystem is under influence of the three different forces, the spring force that effects the closing of the actuator, the magnetic force causing

the triggered motion of the actuator and the other external forces of the plunger. The characteristics of the motion may vary depending on these relationships.

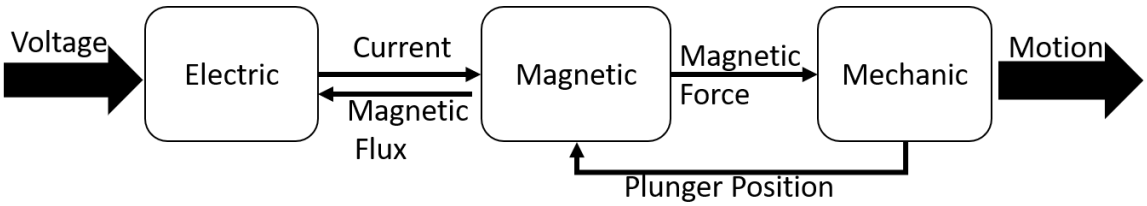

Figure 8: Interlinked subsystems in a solenoid actuator

3.1.1 Electrical subsystem

The electrical subsystem of the solenoid actuator consists of the coil. The lower the resistance, the faster and more current can be applied to the coil. High current causes acceleration of motion. Design of the coil determines the electrical resistance and strongly impacts the inductance of the coil since the inductance formula is given below [20]:

$$\mathcal{L} = \frac{N^2}{R_z} \tag{1}$$

where R_z is total magnetic reluctance, N is the number of coil turns, $\mathcal{L}$ is inductance which is a function of the part's position. The electrical time constant t_v specifies how fast current can rise in the coil.

$$t_v = \frac{\mathcal{L}}{R} \tag{2}$$

where R is resistance. This formula shows that the low-resistance coil is more appropriate for this study. When the temperature change is ignored, the resistance of the coil can be calculated simply as:

$$R = \frac{\rho N(r_{orc} + r_{irc})}{r_{wire}^2} \tag{3}$$

where, ρ is resistivity of copper coil, r_{orc} and r_{irc} are outer and inner radius of the coil, respectively, and r_{wire} is the copper wire radius.

The electrical subsystem can be written as:

$$V = Ri + \mathcal{L}\frac{di}{dt} + i\frac{d\mathcal{L}}{dx}\frac{di}{dt} \tag{4}$$

where V is the voltage, i is the current of coil. Electrical subsystem can be modeled as an RL circuit, consisting of inductor and resistance in series.

The current changes are shown by (5):

$$i(t) = \frac{V(1 - e^{-Rt/\mathcal{L}})}{R} \tag{5}$$

As the plunger moves the inductance will change, hence changing the current over time. The magnetic field and force are determined by current and number of coil turns (NI), Ampere's law states that the current produces the magnetic field. The system is supplied with DC voltage and current rises according to the properties of the coil, such as resistance and number of coil turns. In some coils, the current rises very quickly because the resistance of these coils is quite low. If the low-resistance coil and the slow magnetizing material are combined, then the current reaches the steady-state before the motion is completed. Often the current does not reach the steady-state value before the plunger completes its motion.

3.1.2 Magnetic Subsystem

When the voltage applied in the solenoid, magnetic flux will appear inside of the solenoid as shown in Figure 9. Magnetic aspect of the electromagnetic subsystem of the injector consists of a magnetic circuit that comprises at least one closed path containing a magnetic flux. Magnetic flux refers to the path through high permeability materials such as some soft magnetic materials. If the path has an air gap, the magnetic circuit follows the shortest of the air gap way.

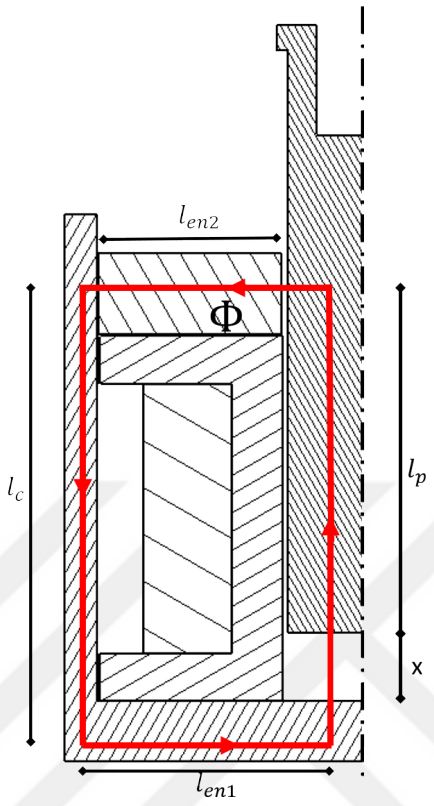

Figure 9: Magnetic flux in the solenoid and case length (l_c), plunger length (l_p), yoke wall length (l_{en2}), radius of case (l_{en1}) and air gap (x) remaining in the magnetic circuit

In the Figure 9, the red line is the magnetic flux, crossing through the plunger and the casing. The role of magnetic material in the amount of flux produced will be described. From Figure 9, the generated magnetic flux seems to pass through four reluctance.

$$R_z = R_c + R_y + R_x + R_p \tag{6}$$

where R_c is the reluctance of the casing, R_y is the reluctance of the yoke, R_x is the reluctance of the air gap and R_p is the reluctance of the plunger.

$$R_z = \frac{l_c}{\mu_0 \mu_r A_c} + \frac{l_{en1}}{\mu_0 \mu_r A_{en1}} + \frac{l_{en2}}{\mu_0 \mu_r A_{en2}} + \frac{x(t)}{\mu_0 A_{pl}} + \frac{l_{p(t)}}{\mu_0 \mu_r A_{pl}} \tag{7}$$

where l_c, l_{en1}, l_{en2}, and l_p dimensions are shown in Figure 9. Length x is the air gap. A_{pl} is the cross-sectional area of the plunger which is perpendicular to the flux path. A_c, A_{en1}, and A_{en2} are the effective area of case thickness, case bottom, and yoke where the flux is crossing, respectively. In the magnetic circuit, the length of the plunger and the air gap vary over time. As the plunger moves in the direction of closing the air gap, the length of the plunger in the magnetic field increases while that of the air gap decreases. This relationship is shown in equation 8.

$$l_p(t) = l_p(t = 0) + (x(t = 0) - x(t)) \tag{8}$$

Magnetic permeability depends on the material. The symbol of permeability is μ, which is found by multiplying relative permeability μ_r by vacuum permeability $\mu_0 = 12.5\text{x}10^{-7}$ H/m.

The magnetic subsystem can be written as [20]:

$$\Phi = \frac{Ni}{R_z} = \int BdS \tag{9}$$

where B is magnetic flux density, S is a closed surface, Φ is the total magnetic flux in Weber. The reluctance method is a way of using Ampere's law to solve for magnetic field and the magnetic flux of the solenoid.

$$F_{mag} = \frac{\Phi^2}{2\mu_0 A_{pl}} \tag{10}$$

where F_{mag} is magnetic force.

3.1.3 Mechanical Subsystem

The mechanic subsystem consists of the plunger and spring, which can be modeled as a single degree of freedom mass-spring-damper system. The equation of motion is given as:

$$m\ \ddot{x} + c\dot{x} + k\ x = \ F_{mag} \tag{11}$$

where m is the mass of plunger, $\ddot{x}$ is an acceleration, c is a damping coefficient of system, $\dot{x}$ is the velocity of plunger, k is a spring constant, and x is a displacement. $\ddot{x}, \dot{x}, x$, and F_{mag} are the function of time. The effect of gravity is ignored because the system is modeled horizontally.

3.1.4 Finite Element Method Approach

It is difficult to calculate the outcome of the solenoid analytically. Because the equations of solenoid actuator are implicit and have many nonlinearities. FEM is a tool used to solve a wide range of research and industrial problems, including electrical and magnetic field problems, like electromechanical actuators. The FEM for computational electromagnetics can be derived using the basic principle of energy conservation. Therefore, the operation of the solenoid actuator is examined using finite element software. Some software is specialized to solve electromagnetism, such as ANSYS Electronic Suite. ANSYS Electronic Suite can solve the static and transient behavior of a solenoid. In time-dependent analyses, magnetic field properties and motion behavior were obtained by applying direct current to the solenoid coil. The electromagnetic force is calculated by Maxwell stress tensor as shown below:

$$\vec{F}_{mag} = \iint \left\{ \frac{1}{\mu_0} \left(\vec{B}.\vec{n} \right) \vec{B} - \frac{1}{2\mu_0} \vec{B}^2.\vec{n} \right\} ds \tag{12}$$

where n is a unit vector pointing out of surface.

Permeability is given with the relationship between magnetic field strength and magnetic flux density.

$$B = \mu H = \mu_0 \mu_r H \tag{13}$$

where H is magnetic field strength, H cannot be defined with a single value for the

whole solenoid. Because every point on the solenoid actuator that is analyzed has a different value. To find the magnetic flux density, the magnetic field strength is multiplied by the permeability of the material at that specific point.

3.2 Used parameters FEM Analysis

A solenoid actuator is designed and manufactured to work slowly to better understand the movement of the solenoid actuator. Solenoid actuators require an optimal design due to the complexity of design parameters. While the dimensions of the solenoid actuator parts to be used in aerospace applications where weight is of great importance should be as small as possible, the cost and ease of manufacturing are important for mass production, while many other applications it is desirable to consume minimum energy.

Solenoid actuator's characteristics were determined to be used in the transient finite element analysis (FEA). These are the resistance of the coil, supplied voltage, the mass of the moving part, spring's stiffness constant, and material parameters of the plunger. According to these parameters, the analysis was completed with the ANSYS Electronics software. The FEA is repeated with many materials with unique B-H curves. The purpose of the analyses was to determine the material combination that provides the difference of actuator opening time.

3.2.1 Electrical Parameters

The magnetic field and force are determined by current and number of coil turns (NI), Ampere's law states that current produces the magnetic field. The system is supplied with DC voltage and current rises according to the properties of the coil, such as resistance and number of coil turns. In some coil, the current rises very quickly because the resistance of these coils is quite low. If the low-resistance coil and the slow magnetizing material are combined, then the current reaches the steady-state before the motion is completed. Often the current does not reach the steady-state

value before the plunger completes its motion. In all experiments, 24 VDC was applied to solenoid. The solenoid actuator coil is designed and manufactured. The coil resistance is 13.3 Ohms and it is measured by FLUKE 179 True RMS Multimeter. Manufacturer supplied the number of turns information which is 650.

3.2.2 Magnetic Parameters

In most cases, the relative permeability is nonlinear which can be seen from the B-H curves of the materials. In the experiment, the material for solenoid actuator plunger, case, and yoke is 430-grade stainless steel.

3.2.3 Mechanical Parameters

The mass of the plunger used in this study is measured as 11 grams. The spring of the system is used to move the plunger back to its starting position. Spring's stiffness constant is experimentally determined for analysis. An OptoForce HEX-70-CE-2000N 6-axis force/torque sensor was fixed next to a linear stage that carries the solenoid actuator. Spring is initially pre-compressed inside the bobbin attached to the plunger. The plunger is moved with 0.1 mm displacements pushing against the force sensor and measurements are recorded. A line is fit to the data and the slope is calculated as 102.6 N/m which is the spring constant.

3.2.4 FEM Analysis with Different Material

Parametric analyses were performed on the solenoid with different plunger materials. Variables other than the material properties are kept constant, such as the spring's stiffness coefficient, supply voltage. Same time steps are used to repeat the analyses. Different materials can be used for different purposes. For example, the plunger's motion time must be very short for an injector mechanism. But the motion time does not necessary to be very short for a lock mechanism. If the motion time is not important, it is necessaring to choose different parameters such as accessibility,

machinability, or material cost. The B-H curves mean magnetization tendency of the materials used in the analyzes. Figure 10 shows the values of 75 different soft magnetic steels in ANSYS Electronic Desktop material library on a single graph [19]. These curves are prepared by combining the values obtained from the experimental data by material dealers or researchers. It is difficult the express B-H curves of materials with equations in high accuracy. B-H curves represent relative magnetic permeability. Red lines are selected soft magnetic materials for parametric analysis. Selected materials are those that have different tendencies, especially from ordinary soft magnetic steel.

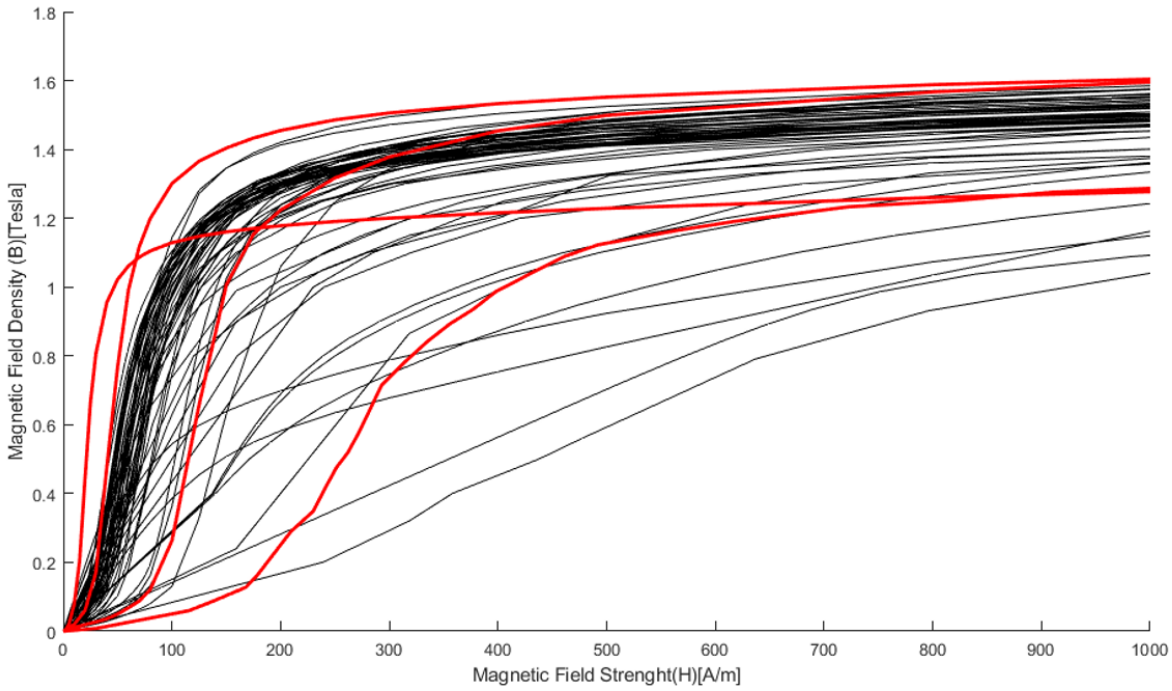

Figure 10: Magnetic tendency of soft magnetic steels on Ansys Electronic Desktop Material Library [19]

Different materials can be used depending on the desired closing times. The names of the selected materials are 430, SuperCore 10JNEX900, 50JN1000, and 50JNA350. B-H curves of these materials are shown in Figure 11.

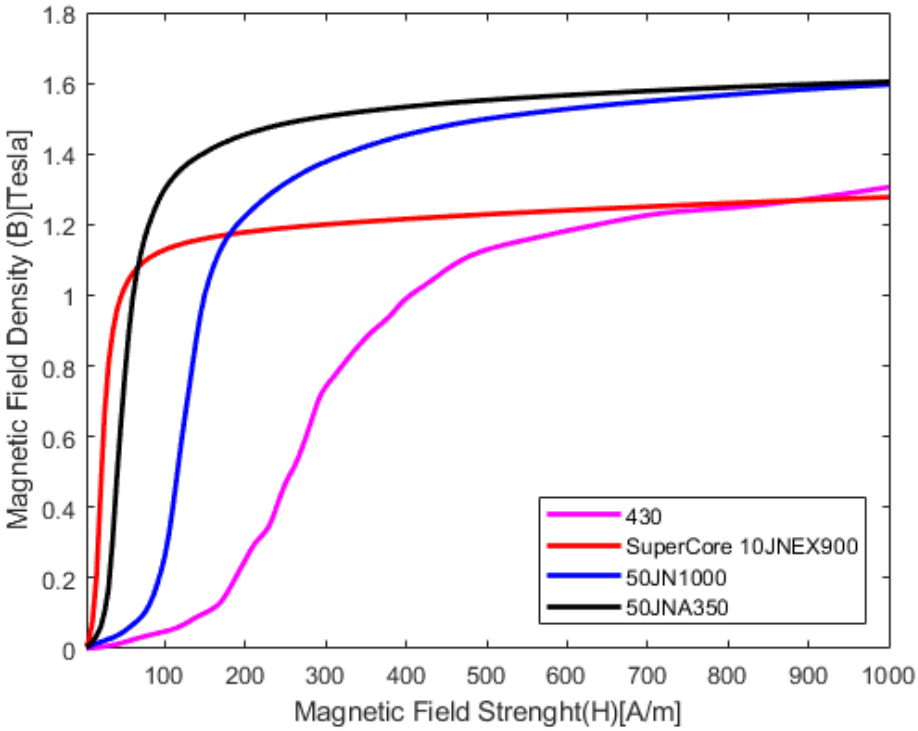

Figure 11: B-H curves of 430, SuperCore 10JNEX900, 50JN1000, and 50JNA350 [19]

"Supercore 10JNEX900" was chosen because it is the material that generates the fastest magnetic flux in the lowest magnetic field. "50JN1000" and "50JNA350" materials were chosen because the flux profiles were distinctive in low magnetic fields even though the saturation points were high and very close to each other. "430" steel was chosen because it can be tested easily and has a low magnetization character.

Once the analysis is verified with the initial material, the analyses of different materials are conducted, and results are shown in Figure 12. The difference between these analyses is due to the tendency of the material to magnetize.

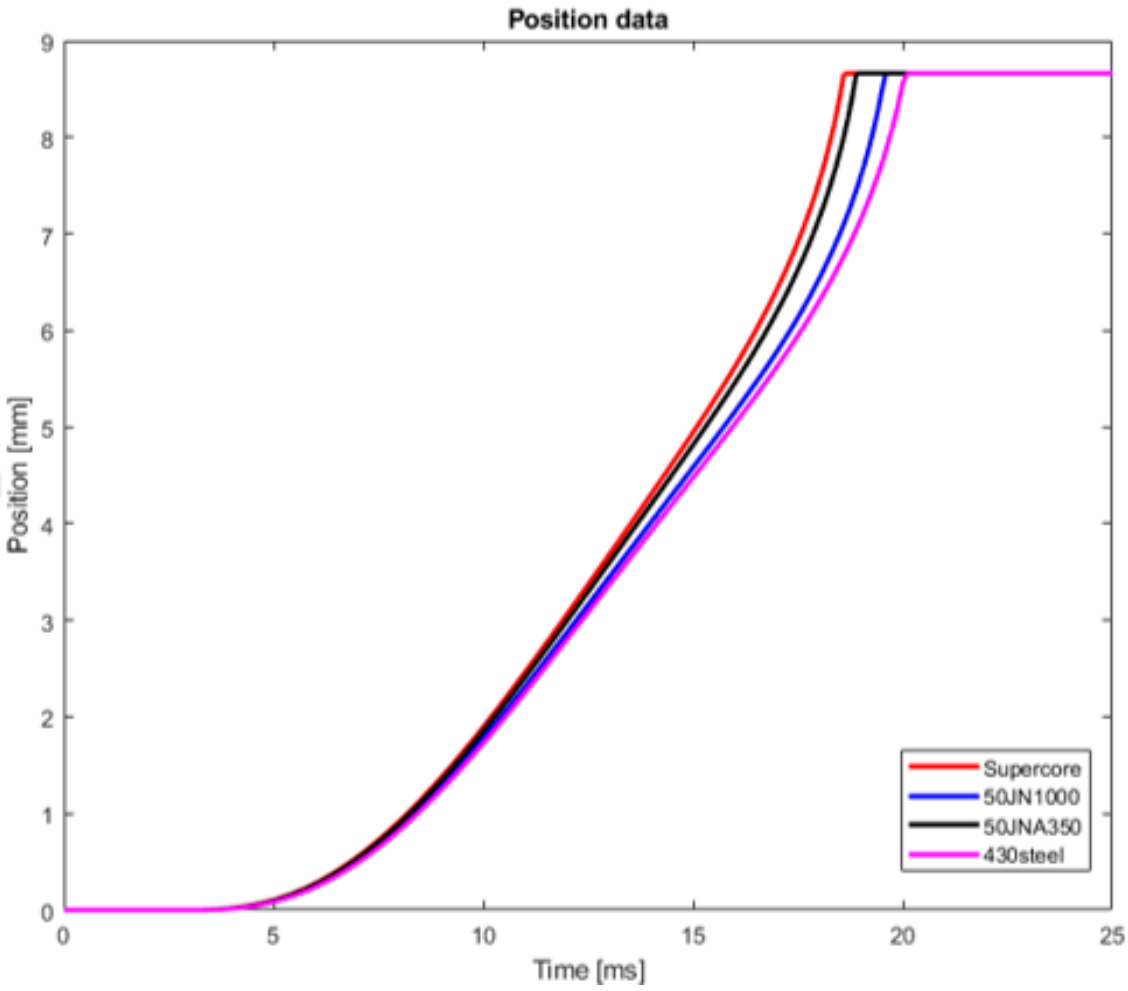

Figure 12: Displacement of 430, SuperCore 10JNEX900, 50JN1000, and 50JNA350 of actuator

The closing time is the time that passes from the start of the voltage supply until the plunger reaches its target. In our study, the closing times of the materials were compared. Supercore material performed 7.4 percent better than the commonly used "430-grade steel". Since the gradient of the "Supercore 10JNEX900" is larger than that of the "430", that is, because it has more magnetic field density at low magnetic field strength. The "Supercore 10JNEX900"s motion finished earlier than the others. The main reason for this is that even though the magnitude of the magnetic field strength is near to zero, the magnetic field generated is larger than the

other materials.

To solve the magnetic field in a solenoid, a finite element model of that solenoid should be developed. Finite element model has four components. These are meshed geometry, material, excitations, and boundary conditions. If the geometry is already drawn in CAD software, finite element software can prepare the mesh model. In the transient electromagnetic analysis, the dynamic mesh was used for the changing position in which the plunger moves. The mesh profiles are shown in the Figure 13 according to the position of the plunger.

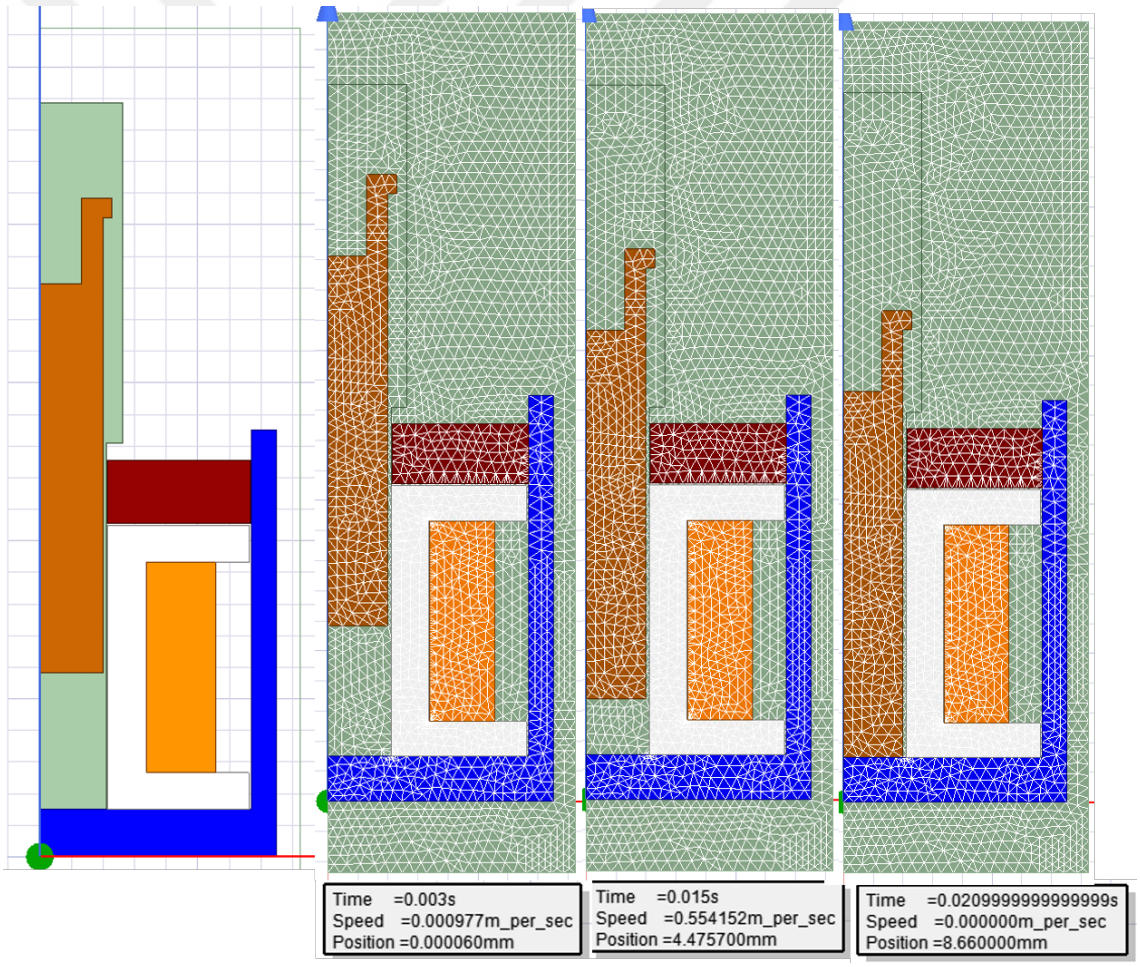

Figure 13: Cross section view of solenoid actuator and mesh profiles of solenoid are shown over position. Respectively, starting the motion, in the middle of the movement and at the end of the movement

The material is the most important factor forming the magnetic circuit by regulating magnetic permeability. Excitations may be related to the voltage and current supplied to the solenoid for magnetic fields. Boundary conditions must be defined. Once these parameters are defined, the FEA can be performed. Electrical, magnetic and mechanical parameters are defined in software. An analysis model was prepared for a transient solution. Magnetic field analysis of the solenoid actuator was performed using 2D axisymmetric solver. Figure 14 shows right-hand side of the solenoid model, the left boundary is specified with an odd symmetry condition. The magnetic flux is isolated from the other three surfaces. In the analysis, the solution time step was 0.1 milliseconds.

The magnetic flux density field results are shown in Figure 14. The magnetic flux density builds up in the plunger over time. As the air gap decreases during movement, the magnetic flux density passing through the magnetic circuit increases. During and after the movement, a maximum magnetic flux density of approximately 1.6 Tesla occurs in the plunger since 430 steel reaches its magnetic saturation limit. Hence, the plunger is shown red in Figure 14. Figures showing the magnetic flux densities of other materials are available in Appendix B.

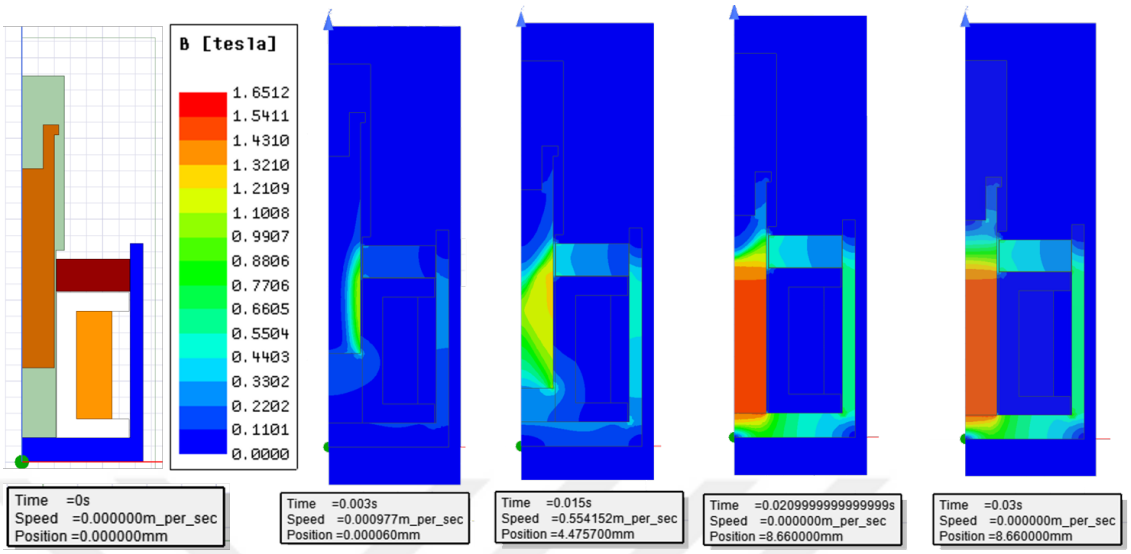

Figure 14: Cross section view of solenoid actuator and magnetic flux density of 430 steel solenoid are shown over time. Respectively, starting the motion, in the middle of the movement, at the end of the movement and in 30 milliseconds

3.3 Experiment, Validation and Results

Experiments were conducted to verify the results of the simulations. National Instruments cRio supplies and digital I/O module (NI9472) the operating voltage to the solenoid actuator. The voltage level is controlled by a Labview program from the control PC. The armature motion is limited to 8.66 millimeters to match the simulations. A high-resolution rotary encoder is used to measure the linear position of the plunger. The linear motion of the plunger is converted to rotary motion with a capstan-rope system. Position encoder reads the movement of the plunger and provides position data. The position data is read by Quanser Q8 and logged on PC with Simulink program. To prevent time and sample rate differences, NI cRio sends a synchronization pulse to Quanser Q8. This pulse is used for finding magnetic charging time which is the delay between the actuation signal and the start of the movement. The instantaneous change of the current was measured with KEYSIGHT 1146B current probe. The 1146B current probe allows accurate measurement of currents from 100mA to

100 A without disturbing the circuit [36].

The results of the experiment show that the armature of the solenoid actuator starts its motion 3 millisecond after the voltage is supplied to the system, and it takes about 17 milliseconds to reach its final target position. As shown in Figure 15, the motion of the tested solenoid actuator matches the simulation data. There is an oscillation where the plunger reaches the target position in the experiment in 21 millisecond. The reason is that the maximum motion is defined as 8.66 mm in the FEA environment and analyses are stopped when the target is reached. But in reality, the plunger hits the target and oscillates before reaching to a stop. As shown in Figure 15, the measured current value is above the current curve of the simulated since the voltage is applied. After a certain current value, the current flow profile becomes compatible. Although the current comparison seems incompatible, the current profiles overlap each other. The simulated results are in good agreement with experiment results when the sensor is in the measurement range.

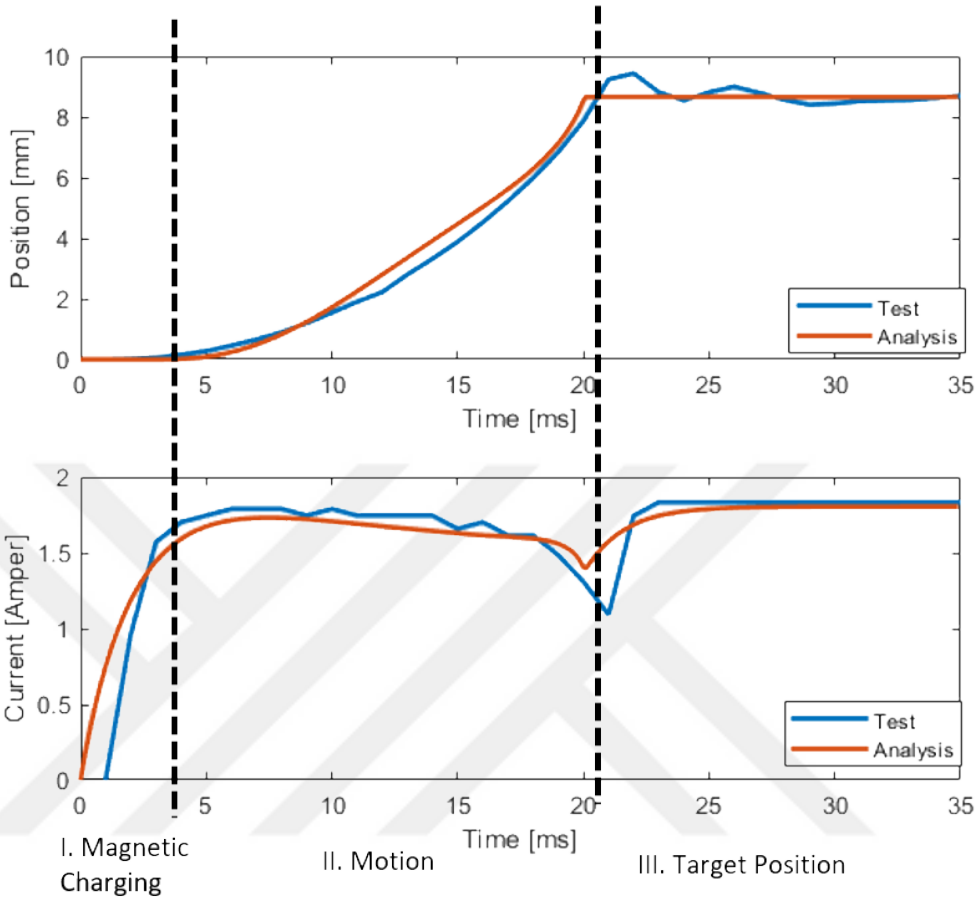

Figure 15: Experiment setup for measured current and position

Transient modeling of the closing mechanism of a solenoid valve is difficult since one needs to solve the nonlinear magnetic, electrical and mechanic equations at the same time. All subsystems affect each other and are also time-dependent. The action can be examined by dividing it into three regions depending on the state of movement: magnetic charging, motion, and target position.

I. Magnetic Charging: In this region, solenoid turns on but there is no movement. There is a current increase in the electrical time constant ratio. Magnetic force is not enough to move the plunger.

II. Motion: Characteristic of the solenoid current is used to determine the movement of the plunger. When the movement starts, the slope of the current changes.

But it can be noticed that the difference between the peak and valley of the solenoid current is due to back electromotive force. Because the plunger's speed suddenly increases too much. The magnetic force increases rapidly because the air gap is very small. When the motion is over, the decrease in current stops.

III. Target Position: In this zone, the plunger is limited from motion by the stopper. Back electromotive force has disappeared and the current continues to increase until it reaches the steady-state

3.4 Summary of Solenoid Mechanisms

In this part of the research, the effect of the plunger material on the motion of the solenoid actuator was investigated. The plunger's displacement is not known in advance as an analytic function of time. The relationship of electromagnetic equations, electric circuit, and the equation of motion has enabled an analysis of the solenoid actuator. Finite element method was applied using ANSYS Electronics. In this method, to simulate the solenoid actuator's magnetic field, a simplified axially symmetric plane model is adopted. FEA is a powerful tool in considering not only the geometric and material nonlinearities but also the dynamic characteristic. The dynamic characteristics of the solenoid actuators are compared to the material. It is shown that dynamic properties of motion can be estimated according to the B-H curve of materials.

In this section of thesis, method for analysis was verified. Thus, each design can be modelled by software before manufacturing, and the physical outputs of solenoid actuator can be predicted.

CHAPTER IV

MODELING AND DESIGN METHODS OF THE SOLENOID BASED INJECTOR

This section describes how to design and model the solenoid based injector. The working principle of an injector can be summarized as high precision and high-speed valve with an actuator. In solenoid based injectors, the electromagnetic coil receives a voltage signal and then the generated electromagnetic force gradually attracts magnetic parts of the armature and overcome the liquid pressure and spring force. Under the electromagnetic force, the armature moves toward the core direction, away from the seat, and fluid is ejected from the spray holes(atomizer) and broken up into small particles which are droplets; when the injection signal disappears after that electromagnetic force is lost, armature moves towards the direction of the valve seat under the forces include fluid pressure, the spring force and the gravity until the needle closes, thus complete a fluid injection cycle.

4.1 Classification of Solenoid Based Injector

The injectors are controlled electronically by a solenoid actuator, which can withstand a fluid pressure. A magnetic field is established when the coil is energized, and then the actuator lifts the needle to open the valve; simultaneously, a metered amount of fuel is injected into the engine. The spray directions and injector opening timings are adjusted according to design and application. When the coil is de-energized, the valve needle(armature) is pressed by spring force back down against the valve seat, and the fuel injection is interrupted.

In this thesis, injectors are examined under two classes according to their designs.

These designs can be named as channel type and pool type which are shown in Figure 16, which are explained in detail below.

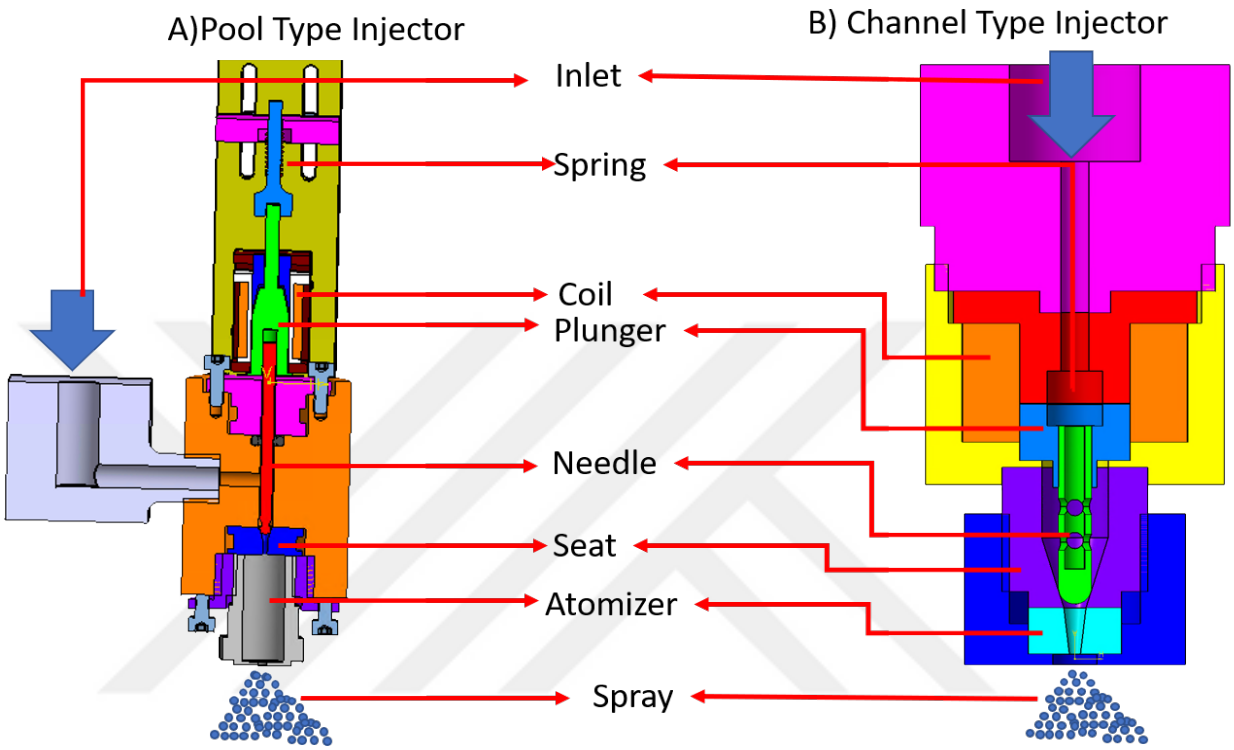

Figure 16: The two types of solenoid based injectors are shown. **Type A**: In a pool type injector, fluid is kept separate from the actuator in a chamber. **Type B**: In a channel type injector fluid passes through the actuator.

4.1.1 Channel Type Injector

Channel type injectors have a compact design. It consists of layers from inside to outside. In the outer periphery there is a housing and inside there is a channel. Liquid passes through the center of the solenoid actuator. The fluid enters the inlet of the injector and passes through the actuator. During the design process of the channel type injector, design improvements have been made. These steps are shown in Figure 17. Since the sealing surface is not movable, it is easier to ensure sealing. This type of injector has more examples in the literature.

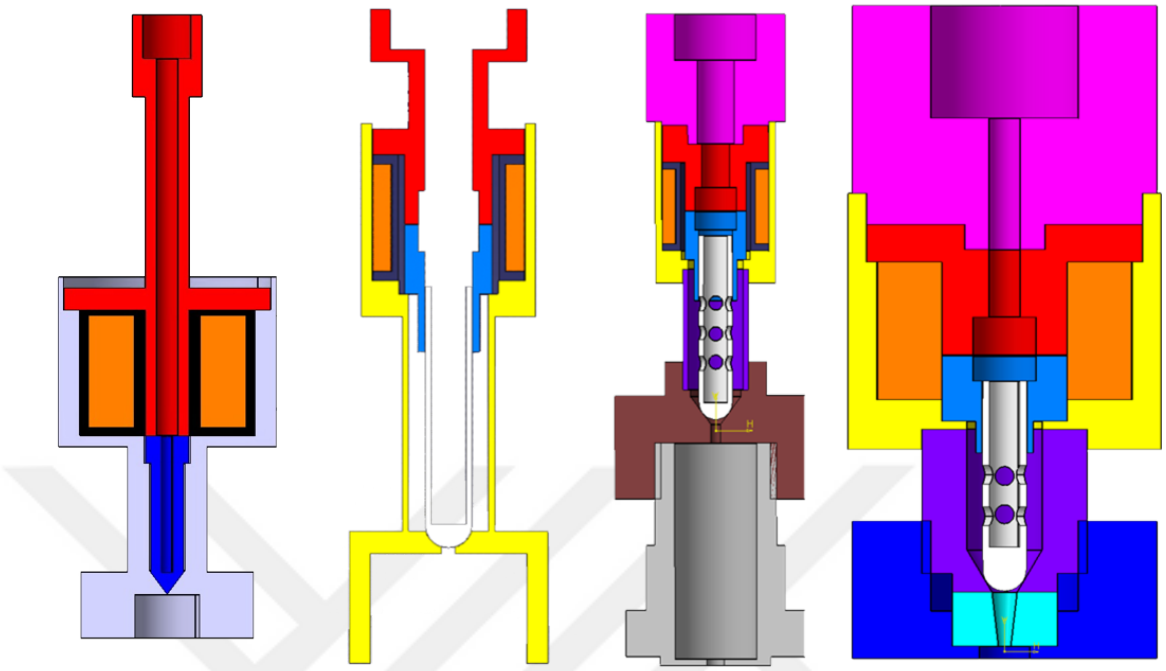

Figure 17: Channel type injector design steps. **Left to right:** General concept of the channel type injector is design given. In second design is scaled down in size. The magnetic circuit of injector is optimized. In the last design, the modularity of the injector is maximized

At first, the objective was to design the solenoid in three parts except for the coil. But when there are fewer parts, magnetic flux leaks in the magnetic circuit. The magnetic circuit, which had to be a rectangular shape around the coil, but this first design caused magnetic leaks in the direction of the needle and the inlet. For this reason, the materials to be included in the magnetic circuit must be a magnetic material, while the parts such as needles and inlet must be selected from non-magnetic materials. This design limits the solenoid actuator materials that may be in the magnetic circuit. Also, the materials must be resistant to oxidation. In addition, this design has been removed due to the fact that transition-fitting methods would be used in assembly and it did not have modular features.

4.1.2 Pool Type Injector

In the pool type injector design, all core elements are separated from each other. Therefore, such designs provide an advantage for modularity. The liquid enters a channel on the side of the needle hole and is collected in a pool away from the actuator. Core elements work together in an injector to let achieve the desired spray ejection. The designed injector allows easy interchanging of the core components and provides many injector configurations for performance optimization. This type of injector with modular parts allows experimental succession in product development as prototypes can be quickly manufactured.

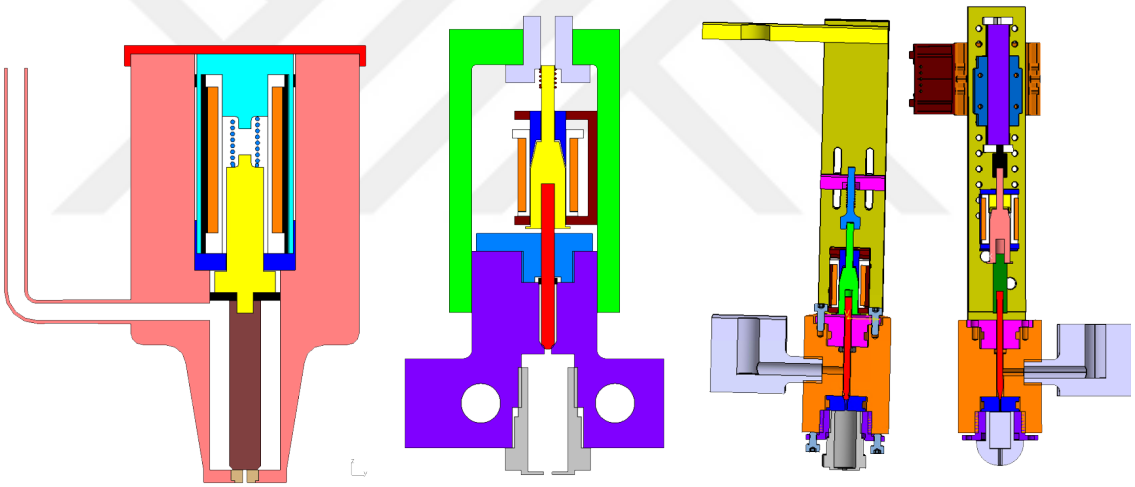

Figure 18: Pool type injector design steps **Left to right:** First, general concept of the channel type injector is design given. In second design a manufacturable injector is designed. In the third version, sealing and alignment of the parts are optimized. In the last version, a position sensor for closed loop control experiments is added.

In Chapter 5, the design and manufacturing steps are explained in more detail. This type of injector has been given priority because it is particularly suitable to create a modular platform. Design versions of the injector are shown in Figure 18.

4.2 Physical Model of the Injector

The relationship between electrical, magnetic, thermal, mechanical and fluid subsystems is depicted in Figure 19. The coupling between these disciplines makes mathematical modeling of the injector non-linear.

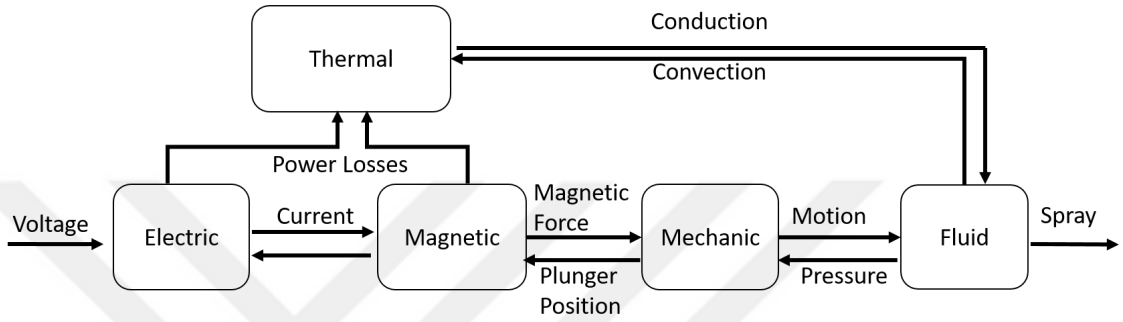

Figure 19: Electrical, magnetic, thermal, mechanical and fluid interlinked subsystems of an injector are shown. A complex connection structure between the injector subsystems exist

The coupling relationship and formation among the electromagnetic, thermal, fluid flow and spray fields was analyzed based on coupling theories. According to the relationship among the different physical fields, coupling models could be established based on the finite element method, and performances of the injector could be analyzed systematically

In the injector system, the voltage must be defined as an input to start the spray. When the voltage to the coil is applied, it creates a time-varying current depending on the coil resistance and coil inductance. The input of the magnetic subsystem is current. Electrical and magnetic effects cause power losses causing heating of the injector. The coil produces heat in proportion to the resistance times the square of the current passing through the bobbin, referred by a phenomenon called ohmic heating. Another phenomenon known as the induction heating is also seen, however, in lesser magnitude compared to the aforementioned. Both of these phenomenons

contribute to power losses and are undesirable. Furthermore, the heat is dissipated by convection with the fluid flowing through the injector and by conduction with parts in contact with the injector.

Depending on the design the used magnetic materials could vary. The current producing the magnetic force highly depends on the magnetic properties of the materials used and the shape and position of the materials.

The mechanical subsystem is subject to three forces, the spring force that effects the closing of the injector, the magnetic force causing the opening of the injector and the pressure force of the liquid that may vary according to the position and shape of the needle. When the plunger moves towards solenoid with the effect of magnetic force, the needle opens the outlet and the fluid is released from the atomizer. The characteristics of the fluid spray vary depending on the inside pressure and geometry of the atomizer [24]. The injector prototype design allows many different atomizers to be tested under the same conditions until the desired droplet size is achieved.

A typical injector consists of coil, plunger, spring, needle, atomizer, and other body parts as depicted in Figure 20. The prototype injector shown is built as a modular unit to test different combinations of core elements. The effects of these parameters by different critical parts have been summarized in the Table 2.

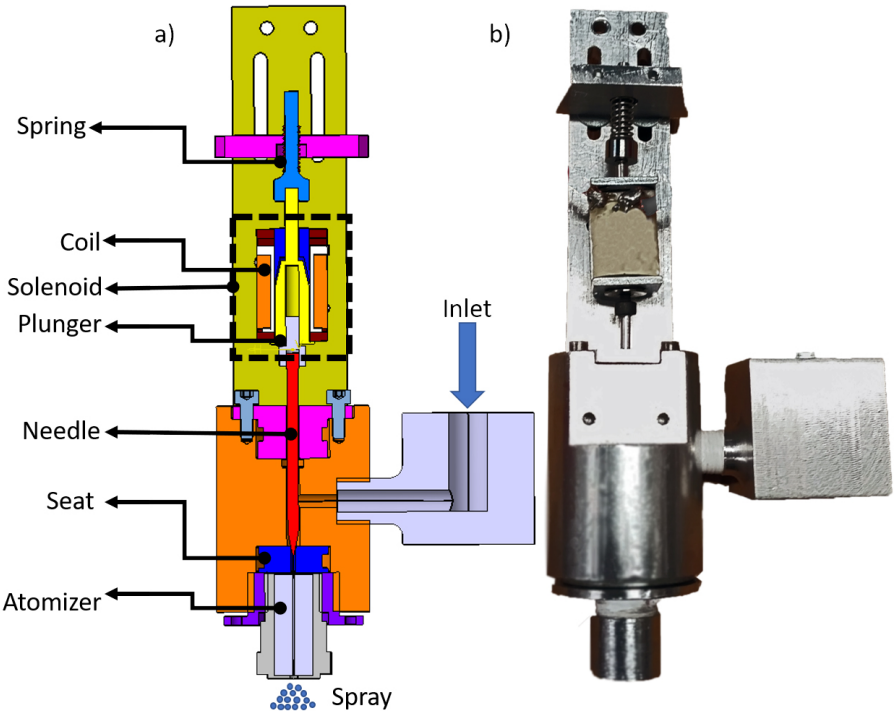

Figure 20: **a**) Cross sectional CAD view of the solenoid based prototype injector **b**) Prototype injector

Table 2: Description of injector Fields and Core Elements

Core Element	**Field**	**Model Parameters**
Coil	Electric	Resistance, current
Solenoid actuator	Magnetic	Material types and part shapes
Spring	Mechanical	Spring stiffness, mass of movable parts
Atomizer, seat, needle	Fluid	Pressure, atomizer specifications, seat-needle coupling
Base, channel, coil	Thermal	Conduction and convection coefficients, power losses

The amount of the sprayed fluid depends on the travel time of the plunger of the

solenoid actuator, which is mechanically coupled with the needle of the injector [37]. Once energized, the solenoid's plunger moves and opens the flow channel for the liquid. Solenoid actuator's pulling power and the spring's stiffness determine how fast the system is opened. Moreover, the dosing quantity depends on the solenoid actuator's displacement and speed. For more precise spray dosing, the design objective is to get the maximum plunger pull force in a short time. Duration of the generated magnetic force can be accelerated by decreasing the coil resistance. However, an abrupt increase in current will overheat the solenoid actuator's coil. Another way to decrease the motion duration is to use a softer magnetic material for solenoid actuator and also by the shape optimization on the solenoid actuator parts. Aforementioned solution is more effective in achieving the maximum amount of force rather than the plunger travel time. When the solenoid is de-energized, the needle moves in the reverse direction due to the spring expansion force. The greater the force of the spring, the faster it closes. If the spring is too hard, it also affects the opening time negatively. The spring is responsible for the closing motion and it provides the necessary force to minimize the leakage from the injector. The needle's shape, inlet pressure, and output pressure also affect the desired electromagnetic force. As the required output pressure may vary according to the cross-sectional area of the injector. The designed modular injector system allows the designer to replace the spring unless satisfactory injector performance is achieved.

4.2.1 Electrical Model

The electrical aspect of the electromagnetic subsystem of the injector consists of the coil. In Section 3.1.1, the electrical subsystem of the solenoid actuator is described in detail. The electrical model of the injector system is essentially the same as the solenoid actuator.

4.2.2 Magnetic Model

Magnetic aspect of the electromagnetic subsystem of the injector is consisting of a magnetic circuit which is comprised of at least one closed path containing a magnetic flux. The magnetic model of the injector can be modeled as a solenoid actuator in Section 3.1.2.

Unlike solenoid actuators, there are some considerations in magnetic modeling of solenoid-based injectors. One of them is related to the choice of material to be used for the solenoid actuator of the injector. Whether the injector will contact the solenoid actuator side is an important criterion because the liquid to be discharged from the injector is corrosive. As the amount of chromium in the steel increases, the magnetic properties generally decrease and corrosion resistance increases [38]. For this reason, injector design is very important in material selection.

Another important difference in the solenoid actuator of the injectors from the standard solenoid actuator is the amount of displacement. The response time of the injectors is expected to be short. The total reluctance of the injectors should, therefore, be very low. The only way to do this is to reduce the stroke distance and ensure that there is no air gap in the magnetic circuit other than the stroke.

4.2.3 Mechanical Model

During the working process of the injector, the needle moves under the action of spring force, hydraulic pressure and electromagnetic force. Needle collides with core or seat in an elastic collision process. So, the highest position when the needle collision with the core is above the given needle lift value. Similarly, the lowest position when the needle collision with the valve seat is below zero [39]. Kinetic model of injector's needle is shown in Figure 21.

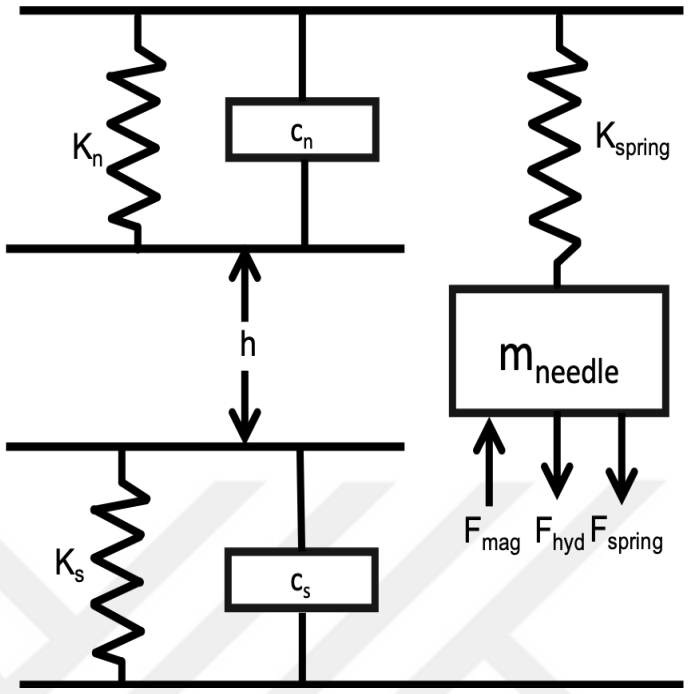

Figure 21: Kinetic model of plunger

The mechanical model can be given as a single degree of freedom mass-spring-damper system. The equation of motion is given as:

$$m\ddot{x} + \dot{x}(c_s + c_n) + (K_s + K_n + K)x = F_{mag}(x) + F_{hyd}(x, \dot{x}) + F_{spring} \qquad (14)$$

where, m_{needle} is the mass of the needle, c_s and c_n is the damping ratios of seat and needle, K_{spring} is spring's stiffness constant, K_s and K_n is the elasticity of seat and needle, F_{mag} is the electromagnetic force, F_{hyd} is the hydraulic force, F_{spring} is spring force, x is the needle position, h is the stroke and t is time. When the needle moves $(0 < x < h)$, $c_s = c_n = 0$ and $K_s = K_n = 0$ and $K_{spring} \neq 0$. And initial conditions are $x(0) = 0$, $\dot{x}(0) = 0$.

4.2.4 Thermal Model

The thermal field as a relevant between the electromagnetic and fluid flow of the solenoid injector which greatly impact on its comprehensive performances. For example, internal combustion engines, the higher fuel temperature is beneficial to generate

smaller fuel droplets and faster evaporation.

Power losses are also important criterions in the design stage, including Ohmic loss, core loss, and solid loss. All of these losses associated with the comprehensive performance of injector.

Ohmic loss, P_{Ohmic}, which is generated in conductors when solving DC current flow problems, is given by the following equation:

$$P_{Ohmic} = \int_{Vol} (\vec{E} \cdot \vec{J}) dVol \tag{15}$$

where $\vec{E}$ is the electric field, J is the electric current density.

Core loss in a soft magnetic material is generated by time-varying magnetic flux. Usually, the core loss has been divided into three components: hysteresis loss, eddy current loss and excess loss. These losses are calculated by using the coefficients (K_h, K_c, K_e) derived from the loss graph. At a given frequency, the core loss is denoted as

$$P_{Core} = K_h B_{max}^2 f + K_c (B_{max} f)^2 + K_e (B_{max} f)^{1.5} \tag{16}$$

where, K_h is hysteresis coefficient, K_c is the eddy coefficient, K_e is the excess or anomalous eddy current coefficient due to the magnetic domain, B_{max} is the maximum amplitude of the flux density, f is the frequency.

Solid loss is the loss of conductor material, both contain source current and eddy current. It is directly proportional to the current density. The solid loss is calculated by

$$P_{Solid} = \frac{1}{\sigma} \int_{Vol} J^2 \cdot dV \tag{17}$$

Where σ the conductivity and J is the conductivity of the material.

Total loss is associated only with the loss density fields of magnetic transient solutions. It derives from the total integrated loss averaged by two consecutive times.

Apart from these, there is also conduction and convection heat transfer in the injector parts [40]. The heat transfer occurs by conduction from the contact of the parts in the injector. Heat conduction is the flow of internal energy from the higher temperature zone to the same temperature as the other zone at a lower temperature by the interaction of adjacent parts. The equation is:

$$\dot{Q}_{cond} = -kA\vec{\nabla}T \tag{18}$$

$\dot{Q}_{cond}$ represents the amount of heat transferred in a time, k is the thermal conductivity constant for the material, A is the cross-sectional area of the material transferring heat and $\vec{\nabla}T$ is gradient of temperature.

Heat energy transferred between a surface and a moving fluid with different temperatures is known as convection. In the injector, considering the liquid to be sprayed, convective heat transfer occurs during transport of the liquid in the channels. The equation for convection can be expressed as:

$$Q_{conv} = h_c A \left|\Delta T\right| \tag{19}$$

Q_{conv} is heat transferred per unit time, A is heat transfer area of the surface, h_c convective heat transfer coefficient of the process, ΔT temperature difference between the surface and the bulk fluid.

4.2.5 Fluid Model

When the solenoid plunger moves, the system which prevents the liquid from escaping is eliminated. This means that when the injection starts, a pressure difference occurs between the inside and the outside of the injector. There is a pressurized liquid outlet from inside to outside. While the liquid exits, it atomizes depending on the pressure difference, the dimensions of the holes and the geometry of the holes [24]. The mass flow rate can be examined with the Bernoulli equation as a fluid model when viewed

at the widest angle to the injector [41].

$$\dot{m} = \rho C_d(\lambda) A \sqrt{\frac{2\,|\Delta p|}{\rho}} \tag{20}$$

where $\dot{m}$ is the mass flow rate, ρ is the fluid density, A is the lift dependent cross-sectional area, λ is flow number and $|\Delta p|$ is pressure difference between inside and outside of injector. C_d is the discharge coefficient which is dependent on viscosity, flow velocity and fluid density only for non-cavitating flow.

4.3 Summary of Injector Modelling

All these models show that the effect of the variables in injector design. The electric model of the injector depends on the characteristics of the coil, just like solenoid actuators. When the magnetic model of the injector is examined, its actuator could be classified as a special type which requires short displacement and fast response. For this, it can be said that the air gaps caused by assembly or design should be minimized in the magnetic circuit. In the mechanical model of the injector, it is explained how to select the spring to prevent leakage and fast closing. In the thermal model, it is mentioned that the high current causes the injector to heat up while reducing the movement time. The source, types and amount of this heating are explained. In addition, convection and conduction and heat transfer are also mentioned. Since the performance of the atomizer is out of the scope of this thesis, only the flow rate of the injector is explained and the spray quality which atomizer is responsible is mentioned. The relationship of all these models with each other is explained in general and it is examined which parameters affect which properties when an injector mechanism is designed.

CHAPTER V

DESIGN FINALIZATION AND MANUFACTURING OF THE SOLENOID BASED INJECTOR

When the mechatronic mechanism of the injector is examined, the most important part is the solenoid actuator that allows the holes which are at the end of the injector to be opened and closed.

When literature is reviewed, it is seen that mostly channel type injectors are used in the industry. However, during the research and development of the injector, it will be difficult to produce this type of injector in different parts. Therefore, the focus is on modular design and the production of an injector mechanism that can be easily inserted and removed from the core elements. Under these conditions, it was decided to produce a pool-type injector. Thus, the core parts of the modular injector can be tested different and independent of each other.

5.1 Injector Design

In line with the aim of the thesis, the cross-section of the first pool type injector design is shown in Figure 22. The force generated by the magnetic field inside the solenoid when the coil is energized, the solenoid plunger is pulled up. As since the plunger is connected to the needle of the injector, it raises the needle, causing the fluid flow to the atomizer. Thus, under pressure, the liquid will come out of the atomizer of the injector. It is aimed to form droplets of the desired amount with fast opening and closing.

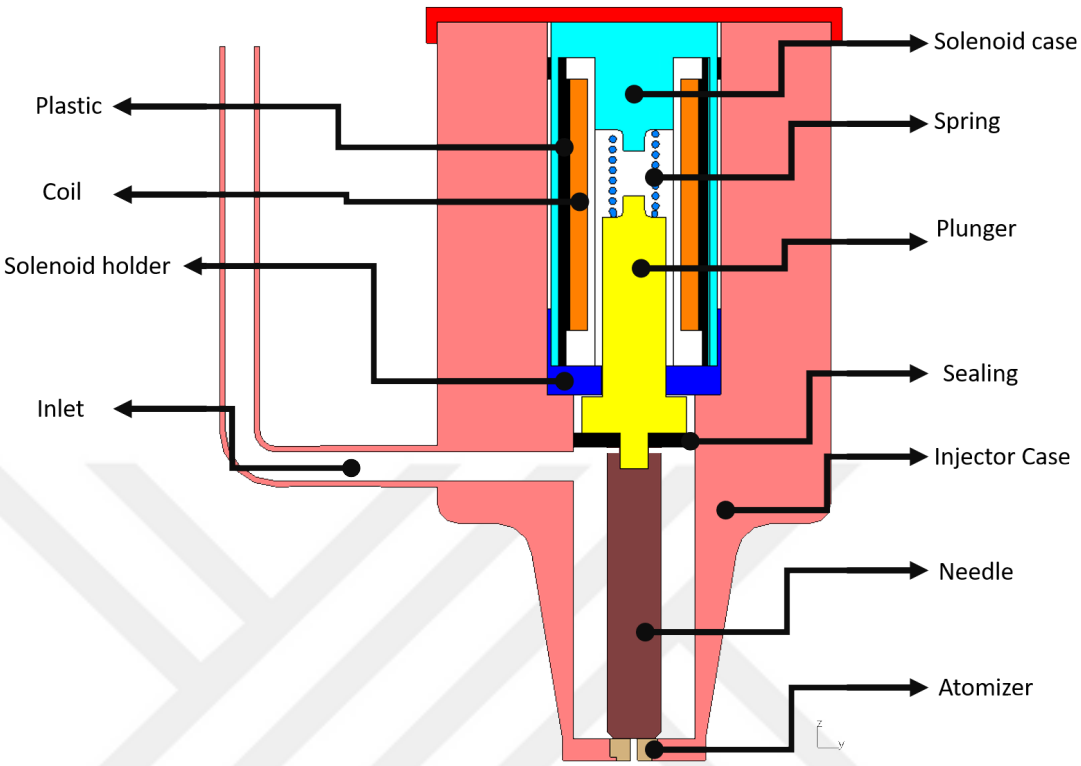

Figure 22: Cross-section of the first conceptual design injector

The design is a conceptual model. Critical design parameters could be determined following the analyzes to be made. Especially on the actuator side, these parameters are the resistance and turning number of coil, case and plunger material, and dimensions of the solenoid actuator. Other important parameters are needle size, spring coefficient, needle-seat compliance, and sealing.

After the injectors were examined and the concept design was made, an injector mechanism which is more suitable for manufacturing was designed. This mechanism is simply designed to control the fluid to the atomizer. As details seen in Figure 23, the plunger of the solenoid actuator is connected to the injector needle. The movement of the plunger also brought the fluid to the atomizer. The prototype was first produced using PLA with a 3D printer and the assembly steps were reviewed. Then it is manufactured from aluminum material using CNC (Computer Numerical Control)

milling. Some wet tests were carried out. During these tests, major problems were encountered especially in terms of sealing. Also, the pool-type injector had problems with axial alignment of parts, as predicted. However, these problems were solved step by step with incremental design improvements.

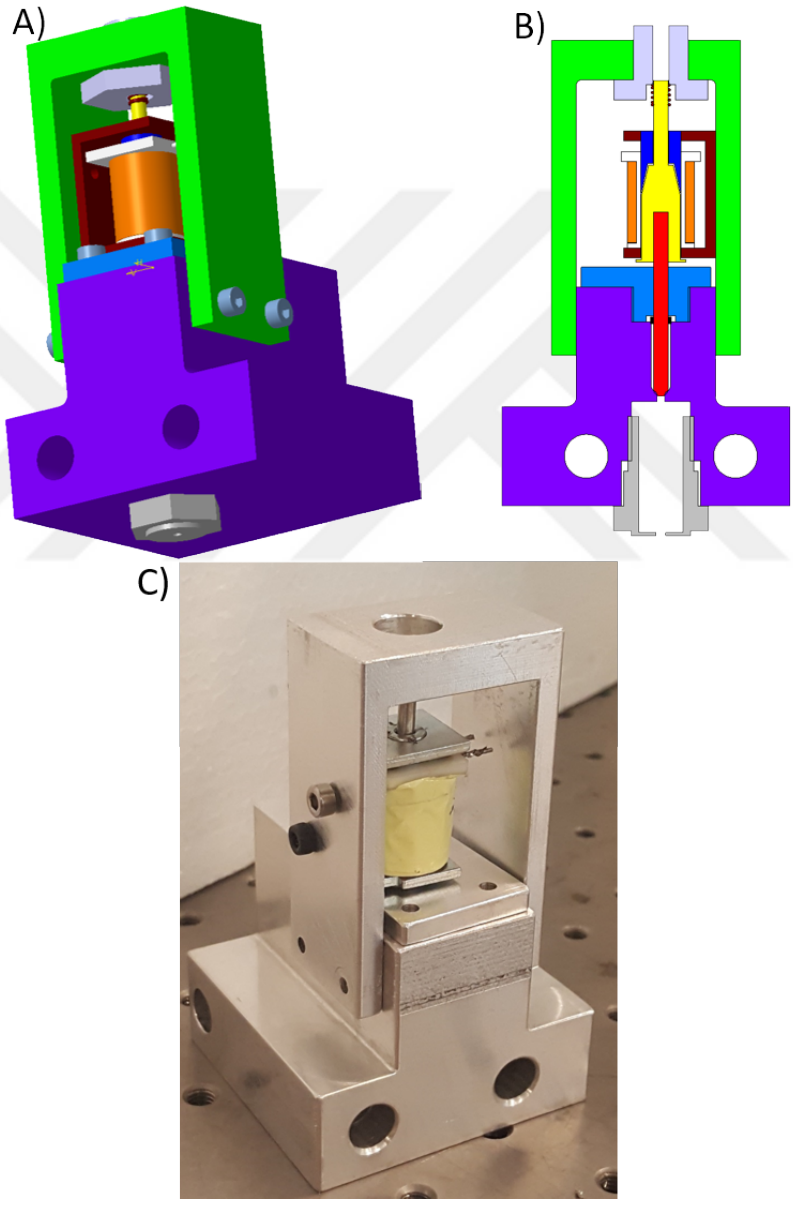

Figure 23: First manufactured prototype. **A)** Isometric view of CAD design **B)** Cross-section of CAD design **C)** Prototype manufactured from aluminum material

5.1.1 Sealing Phenomenon and Surface Roughness

To achieve the high efficiency in spray, the fluid outlet must be carried out only from the injector tip. Moreover, when an undesired leak occurs from any point, the control of the pressure of the fluid is lost. The following equation gives the amount of flow that flows around the moving needle. Estimated leakage can be calculated analytically [42].

$$Q = \pi D \left(\frac{Ua}{2} + \frac{\Delta P a^3}{2\mu_d L} \right) \tag{21}$$

In this equation Q is the amount of leakage, U is the velocity of the needle, a is the gap between the surface and the gasket, μ_d is the dynamic viscosity of the liquid, ΔP is the pressure difference between the two sides of the gasket, L is the length of the working region and D is the diameter of the working region. It is seen that the design parameters are only a, D and L. The gasket must be placed either in the channel to be opened in the needle or the rod as shown in Figure 24.

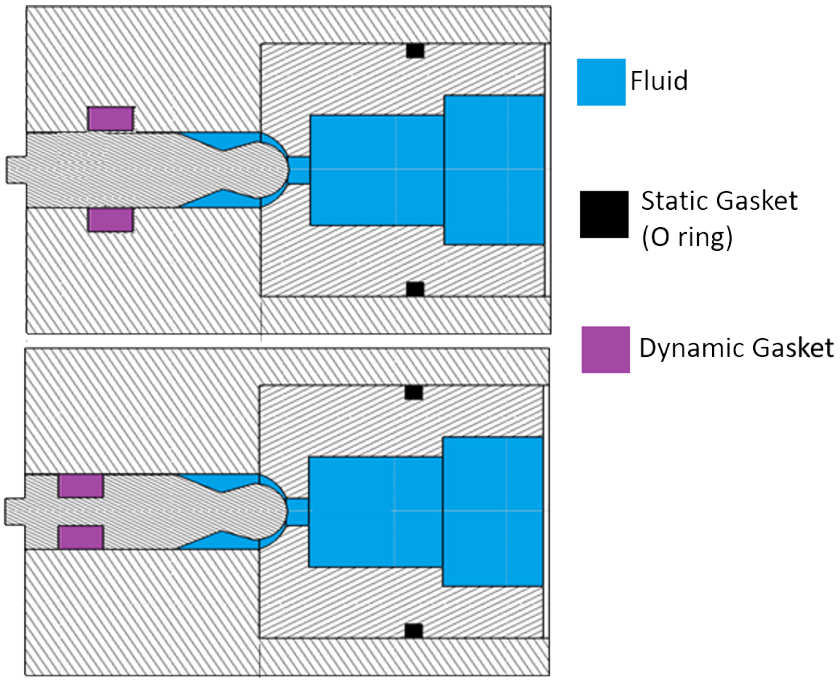

Figure 24: Gasket position options(Upper:Rod Type, Lower:Piston Type)

To reduce the amount of leakage, the surface roughness and the diameter of the working area must be reduced, while the length of the gasket should be increased as much as possible. The first design idea was using the piston type sealing as shown in Figure 25.

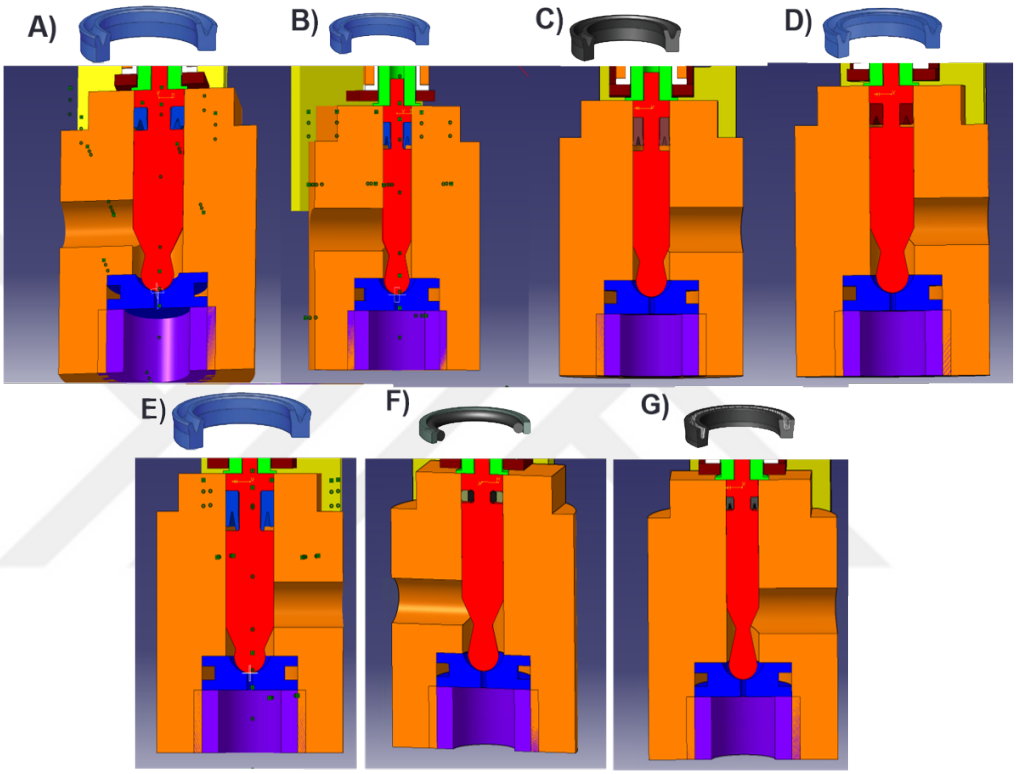

Figure 25: Piston type sealing options

Seven different piston seals were tested in piston type. Type A, B and E are a single acting piston seals designed to have outer lip shorter than the inner lip in order to be used in piston applications. They reduce the risk of leakage from the inner surface. Type C and D are a single acting piston - rod seals and designed to have symmetrical lips in order to be used both for rod and piston applications. Type F is a two-piece double-acting piston seal which consists of a PTFE profile ring and an o-ring as energizing element. Type G is a two piece single acting piston seal which consists of a PTFE u-ring with metal spring as the tension component. All of these gaskets

are the smallest gaskets used for dynamic applications in industry. These designs are made with the idea that it is easier to produce the injector needle by opening the piston needle, rather than opening the groove in the rod in small diameters.

However, instead of grooving the injector needle to reduce the diameter of the working surface, it makes more sense to have the groove on the rod. Considering the difficulties in the production of the needle and the difficulty of grinding operations on the surface of the grooves, it was decided that the rod type design is more reasonable. The design has been changed as in the Figure 26. Besides it is thought that excessive reduction of needle diameter will adversely affect the structural strength of the system. In this design, the piece shown in pink is added to tighten the gasket.

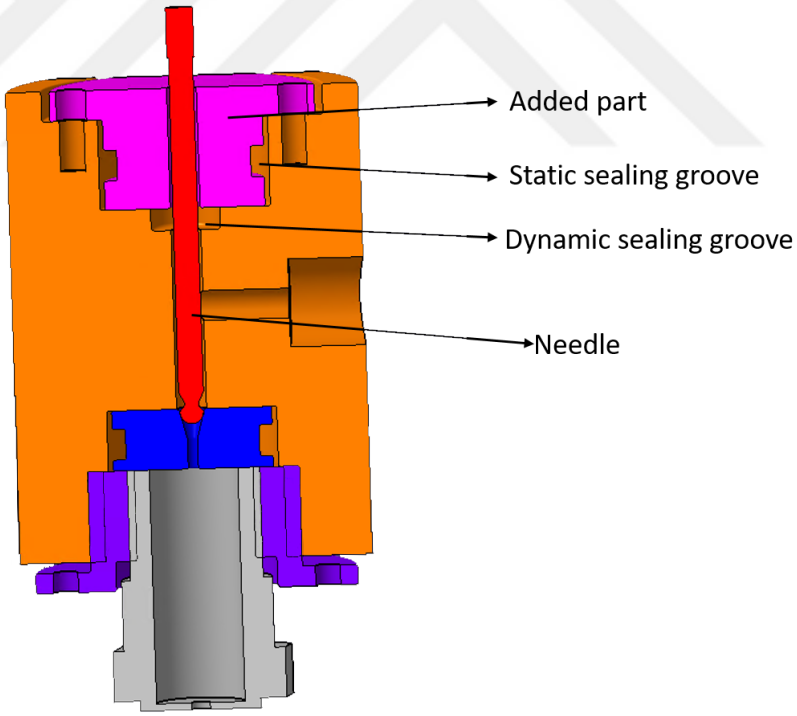

Figure 26: Rod type design for sealing

In addition, the pink and orange parts were drilled from the same point to eliminate axial alignment problems. Since the use of rod seals instead of piston seals would

be more efficient for sealing, it has was to give priority to rod seals despite increasing workmanship and number of parts. In addition, the inner surface of the smallest dynamic seal shall be the working surface. Thus, the diameter of the working surface in the sealing equation was also reduced.

When the gasket catalogs were examined, the minimum dimension of the working surface is 2.5 mm. 2 rod seals were chosen according to this diameter. Gaskets with product numbers K35-0025 and K22-002 in the catalog of KASTAŞ Sealing Technologies Inc. [43] are shown in Figure 27.

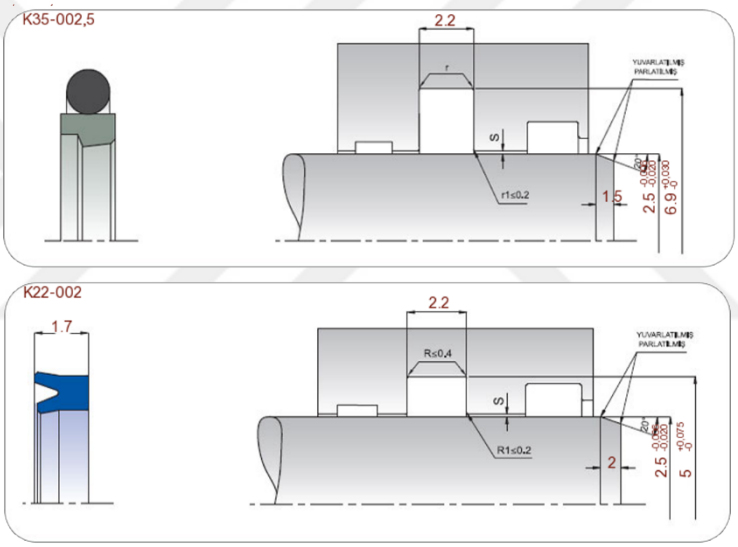

Figure 27: Technical drawings of seals and housings K35-0025 and K22-002 [43]

The working surface must meet two basic requirements. The first one is sealing and the second is to reduce friction force during motion. Of the two seals selected in this sense, the K35-0025 has PTFE material on the working surface, while the K22-002 has NBR material on the working surface. NBR material increases the impermeability by filling the surface roughness. In PTFE material, it facilitates the movement because of the low friction surface area. However, this negatively affects the sealing. The properties of these two materials against surface roughness are shown in Figure 28.

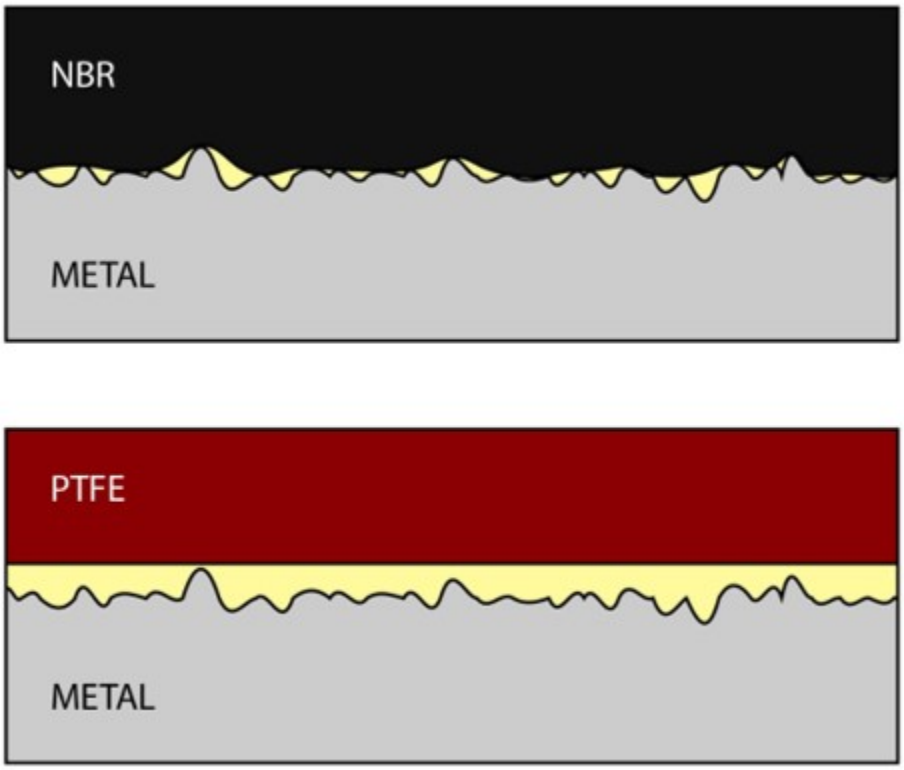

Figure 28: Effect of NBR and PTFE on surface roughness [43]

Surface roughness represents the variable a, which is one of the most important parameters in the leakage equation. It refers to the gap between the gasket and the material. Even a small gap creates a serious leak. To minimize this leakage, in particular, the roughness of the surface between the injector needle and the seal must be minimized. Afterward, the roughness of this surface should be measured. Surface roughness can be expressed in two different values as R_a (arithmetical mean deviation of the assessed profile) and R_z(arithmetic mean of 5 consecutive maximum values at a given surface length). The value R_a is defined as the arithmetic mean of the absolute value of the roughness magnitudes at a given surface length on the surface. R_z is the arithmetic mean of 5 consecutive maximum values at a given surface length. These terms are shown in Figure 29. According to the information in the catalog of the seals [43], the R_a of 0.4 microns is recommended for working surfaces

work with made of NBR material, and the maximum R_a is 0.2 microns for work with PTFE sealing.

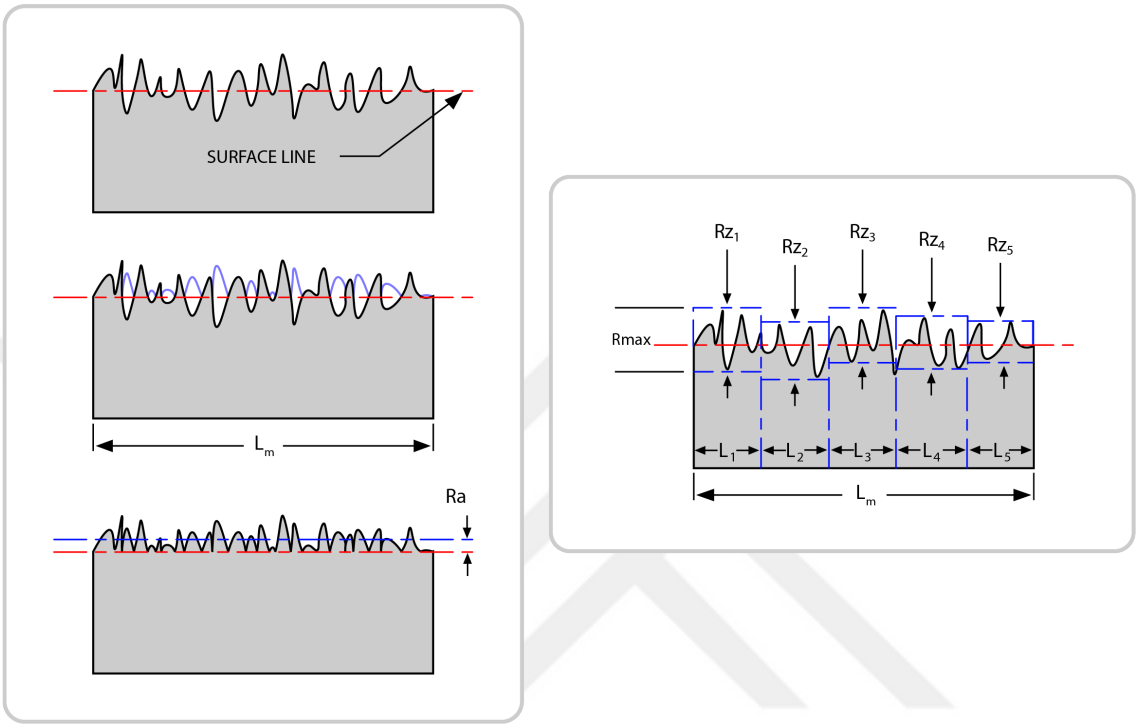

Figure 29: R_z(arithmetic mean of 5 consecutive maximum values at a given surface length) and R_a (arithmetical mean deviation of the assessed profile) paremeters [43]

$$R_a = \frac{1}{L_m} \int_0^{L_m} |z(x)|\, dx \tag{22}$$

$$R_z = \frac{R_{Z1} + R_{Z2} + R_{Z3} + R_{Z4} + R_{Z5}}{5} \tag{23}$$

A number of different methods have been studied to reduce the surface roughness of the injector needle. But the length and diameter of the injector needle were problematic for the polishing methods to be used. Finishing methods generally applied a higher amount of force to the needle than the needle could handle. The most appropriate method was to use fine quality sandpaper. The injector needle was connected

to the manual turning machine and turned at high speeds (1800 rpm). Then, the side surface of the needle was sanded by squeezing it between 2000 grade sanding paper. A measuring instrument called the profilometer was used to measure R_a and R_z values. The model number of the profilometer is PCE-RT-1200.

There is a small protrusion at the end of the moving pipe under the profilometer. This protrusion moves back and forth over the surface to measure the roughness of the surface and display the values on the digital display. Since the profilometer was mainly designed to measure flat surfaces, a different apparatus was needed to measure the surface of the injector needle having a cylindrical surface. A special apparatus is designed and manufactured in 3D printer. In this apparatus, a cavity is intended to accommodate the needle and the needle is intended to remain constant as the measuring probe of the profilometer moves. The experimental setup is shown in Figure 30.

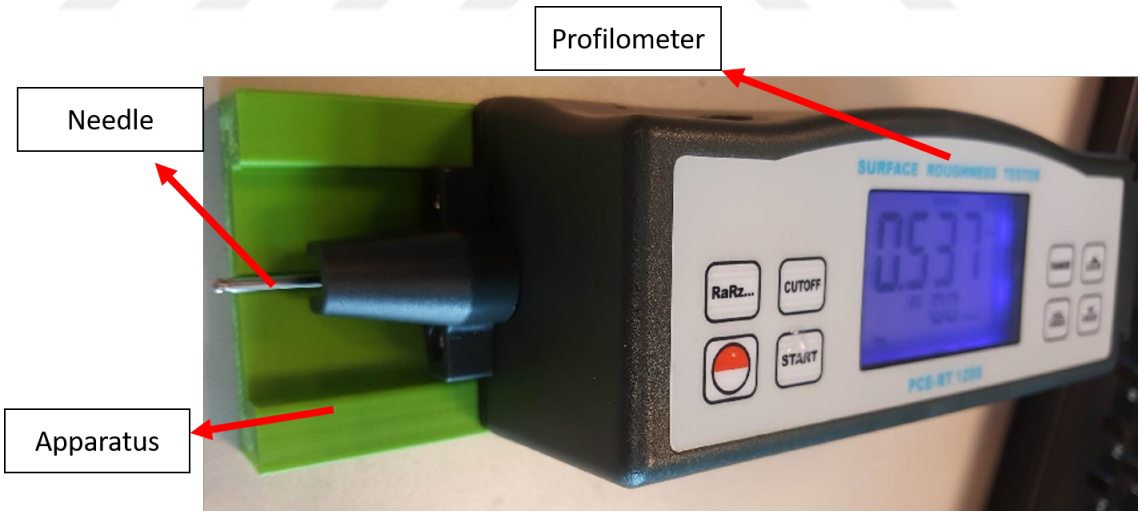

Figure 30: R_z and R_a measurement experiment setup: The needle is inserted into the cavity of the apparatus. Thus, the profilometer detects and measures the side surface of the needle as a flat surface.

R_a and R_z values on the surface of the needle before and after this finishing procedure were measured and recorded in Table 3. In these tests, R_a was measured

at 10 different points and R_z values at 5 different points of each sample. The surface roughness of the side surfaces was measured after samples which are 1,2 and 3 were produced by the lathe. In the 4th and 5th samples, after the lathing process, polishing with high-grade sandpaper was applied as described above.

Table 3: Measured Ra and Rz values

	Rough finish with lathe			**Lathe finish and polishing with sandpaper**	
Needle No	**1**	**2**	**3**	**4**	**5**
Ra1	1.31	1.57	1.701	0.333	0.366
Ra2	1.123	2.075	1.334	0.801	0.465
Ra3	2.066	2.083	1.066	0.313	0.362
Ra4	1.424	2.392	1.432	0.329	0.4
Ra5	1.481	1.977	1.115	0.396	0.352
Ra6	1.993	3.027	1.033	0.315	0.376
Ra7	2.246	3.483	1.318	0.352	0.372
Ra8	1.342	4.232	1.098	0.208	0.054
Ra9	1.587	2.522	1.326	0.233	0.276
Ra10	1.115	2.49	0.765	0.286	0.665
Mean Ra	**1.5687**	**2.5851**	**1.2188**	**0.3566**	**0.3688**
Rz1	5.469	9.506	4.916	0.621	0.854
Rz2	5.306	10.95	7.878	0.577	0.569
Rz3	3.434	10.54	6.673	0.301	1.538
Rz4	4.069	12.33	8.725	0.862	0.606
Rz5	6.055	7.384	4.15	0.455	0.874
Mean Rz	**4.8666**	**10.142**	**6.4684**	**0.5632**	**0.8882**

NBR will be suitable to use as the seal since the mean R_a value reached to 0.4 microns. In addition, the NBR material is more flexible so that it can adapt to the shape of the surface by further reducing the surface roughness effect. Thus, the solenoid based injector is sealed in the dynamic zone.

5.1.2 Manufacturing of the Needle and the Seat

The production of the injector needle and seat was also a challenging problem tested in our prototype. These two parts served as a valve before the atomizer. Again at this point sealing was of great importance. The concept designs for these two parts are shown in Figure 31. In the concept designs, the contact surfaces of the needle and seat were examined. In the first concept, both parts have a conical shape. Thus, the contact surfaces are at maximum level. In the second concept, the needle is spherical, while the seat is conical. In the third concept, the needle and the seat were chosen spherically. In this concept, although the contacting surfaces are good enough for sealing, they are not suitable for axing and manufacturing.

	Geometric Shape of Parts		
Needle	Conic	Hemisphere	Hemisphere
Seat	Conic	Conic	Hemisphere

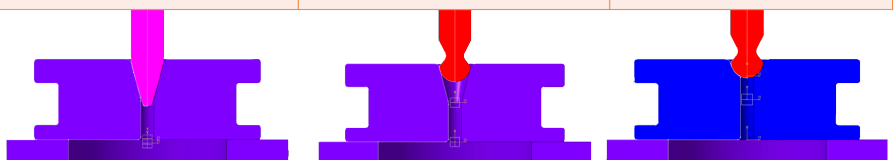

Figure 31: Conceptual design of seat and needle

Considering the length effect of the working region in the sealing equation (21) and manufacturability, it was decided that the most logical choice should be conical in two parts. In order to produce the seat part, firstly the basic shaping of the outer surface was realized by a lathe. 1 mm diameter hole was drilled into the center. Electrical discharge machining (EDM) is a manufacturing process in which the desired shape

is achieved by using electrical sparks. Using the plunge erosion technique from the electrical discharge machines, the material was removed from the seat part where the seat joins with the needle. A copper part was manufactured the needle geometry selected for this process as an electrode mold. The shapes of the copper electrode mold and plunge erosion machine are shown in Figure 32. The seat part is placed on the ground of the plunger erosion machine. The copper electrode mold is also attached to a plunger of the erosion device. The plunger moves to the center of the seat in such away. The hole in the center of seat part thus forms the shape of the copper electrode mold. The seat part can be produced in this manner.

Figure 32: Copper electrode mold and plunge erosion machine (AJAN983)

2.5 mm diameter and the tip of the tapered injector needle manufacturing process in the CNC lathe machine experienced some problems. This kind of problems was not encountered when preparing the copper electrode mold because it is softer than steel. No matter how short the working length is, the axis of the workpiece shifts when the tapered area of the needle is machined. This is shown in Figure 33.

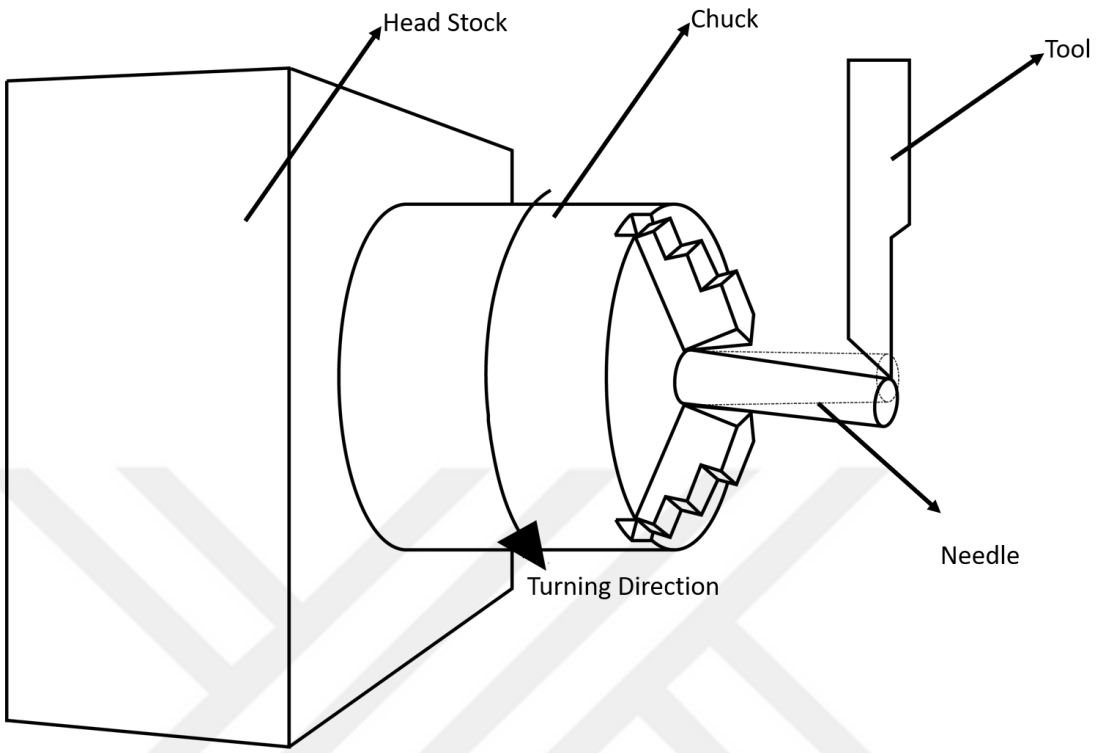

Figure 33: Axis shifting demonstration

This axis shift has some consequences. One of them is the drift on the surface of the lower base of the taper. The trapezoid in the bottom base will be posed a major problem in sealing, as there was a possibility of shifting the seat and needle axis. There were winding-like lines on the worked area of the needle. Again, in this case, it is foreseen that there will be sealing. These problems are also shown in Figure 34

Figure 34: The trapezoid in the bottom base and winding-like lines on the worked area of the needle

To overcome this problem, a special lathe was used to manufacture the needle. The brand and model of this lathe machine is the ANCA MX7 linear axis which is shown in Figure 35. This machine is mainly used for the precise production of turning and milling tools [44]. Thus, very hard and thin parts can be machined with high precision. Therefore, problems in the manufacturing of the injector needle have been eliminated. The needle manufactured as desired is shown in Figure 36.

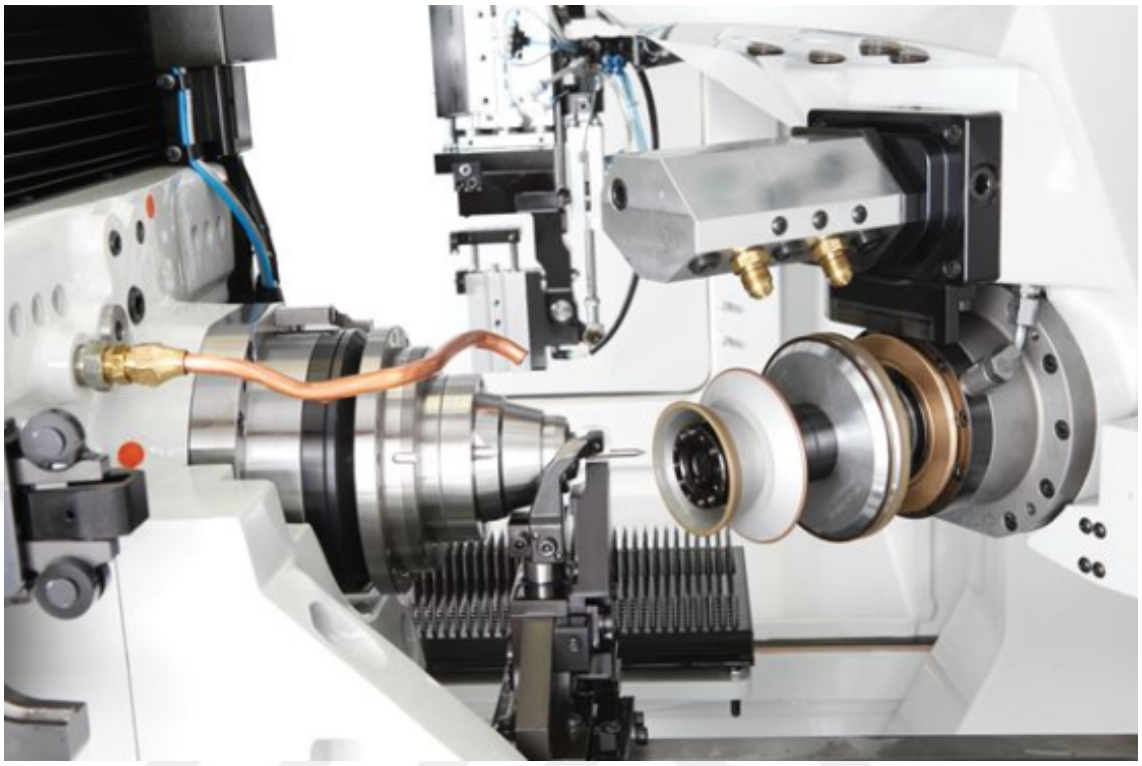

Figure 35: ANCA MX7 linear axis lathe machine [44]

Figure 36: Proper cone shaped needle tip manufactured for the prototype

5.1.3 Assembly of the Injector

Particular attention has been paid to the fact that all parts can be inserted and removed when designing the injector.For this reason, the core parts are designed to be replaced by other models. Parts such as atomizers, springs, needle-seat pairs, solenoid actuators can be replaced at any time. In order to use the solenoid actuator based injector more efficiently, a special control signal must be developed [45]. For this purpose, the position of the plunger of the solenoid actuator must be clearly known in real time. Therefore, encoder and sliding shaft are added to the design. The picture of the designed and produced prototype injector is shown in Figure 37.

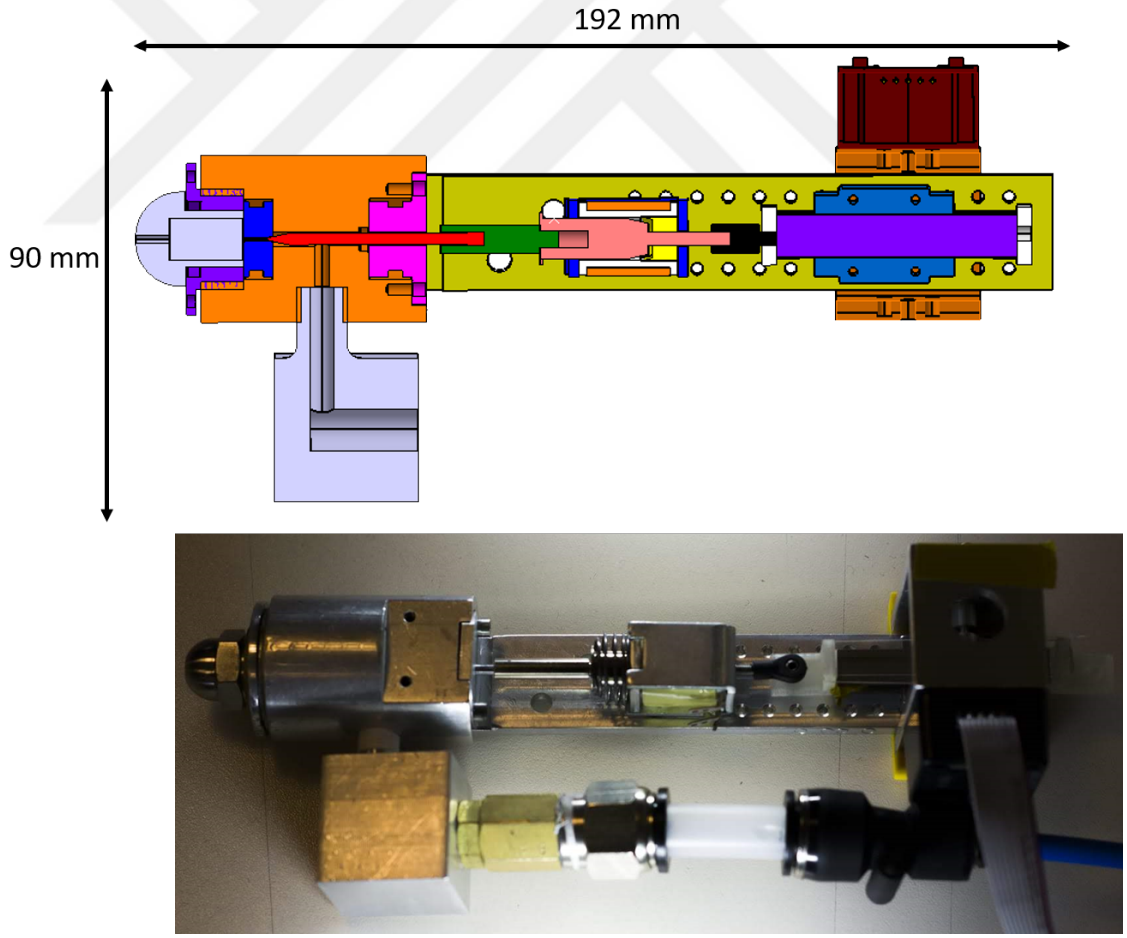

Figure 37: **Top**: CAD design of the injector and **Bottom**: Assembled pool type injector

CHAPTER VI

ANALYSIS AND TESTS OF THE PROTOTYPE INJECTOR

This chapter includes tests and analyses of the operation of the injector. The modular design of the injector system as a whole has been tested for correct operation. These tests initially started with a leak test. Since no leakage problems were observed in the injector prototype, the system is proved that does not leak. Then, magneto-static analysis and verification of this analysis for different solenoid actuators were performed. After that, a test system for determining the characteristics of the springs to be used in the injector mechanism is explained. Finally, the whole system worked together and the time-dependent position change of the solenoid actuator in the injector was measured under liquid pressure.

6.1 Sealing Tests

When designing prototype injectors, one of the most important criteria for correct operation with different subsystems was to ensure that the system was sealed. For this reason, the system has been subjected to sealing tests. When performing the leak test in the first assembly, pressurized fluid is connected to the inlet of the injector with the pressurized fluid tank. It is then observed whether the injector is leaking depending on whether it is open or closed. The environment and stage of this test are shown in the Figure 38.

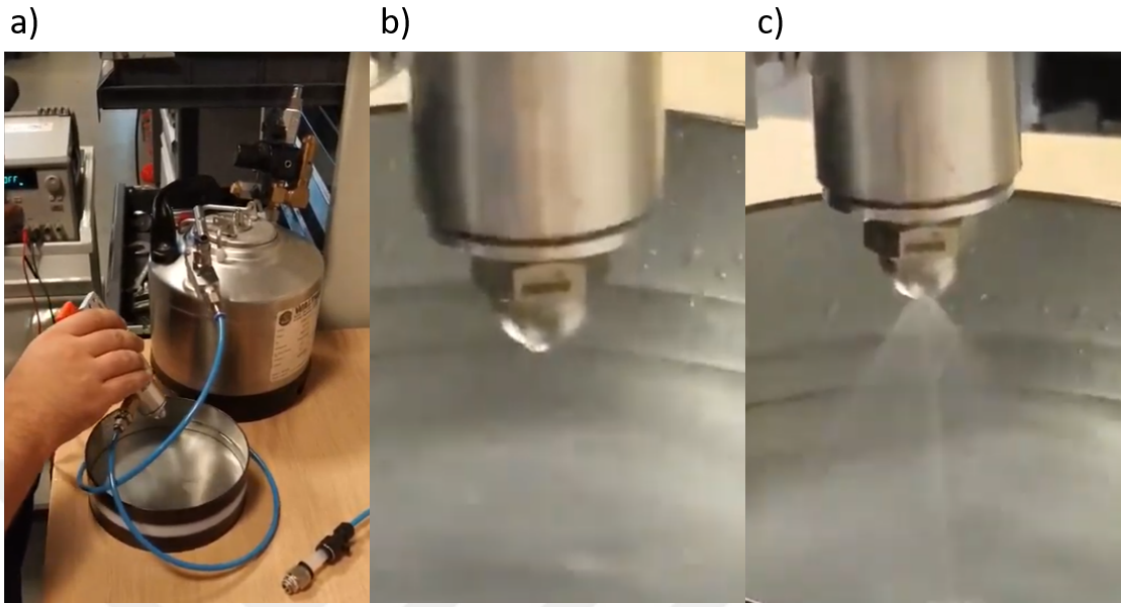

Figure 38: Early stage sealing tests a) Test environment b) Close c) Open

After sealing process, the injector should work with different atomizers and the performance of those atomizers should be observed. For this purpose, it must be connected to a special test system. This test system has special equipment to monitor sprays quality. Laser imaging system and a high frame rate camera system are used to measure these features. The test setup is shown in the Figure 39.

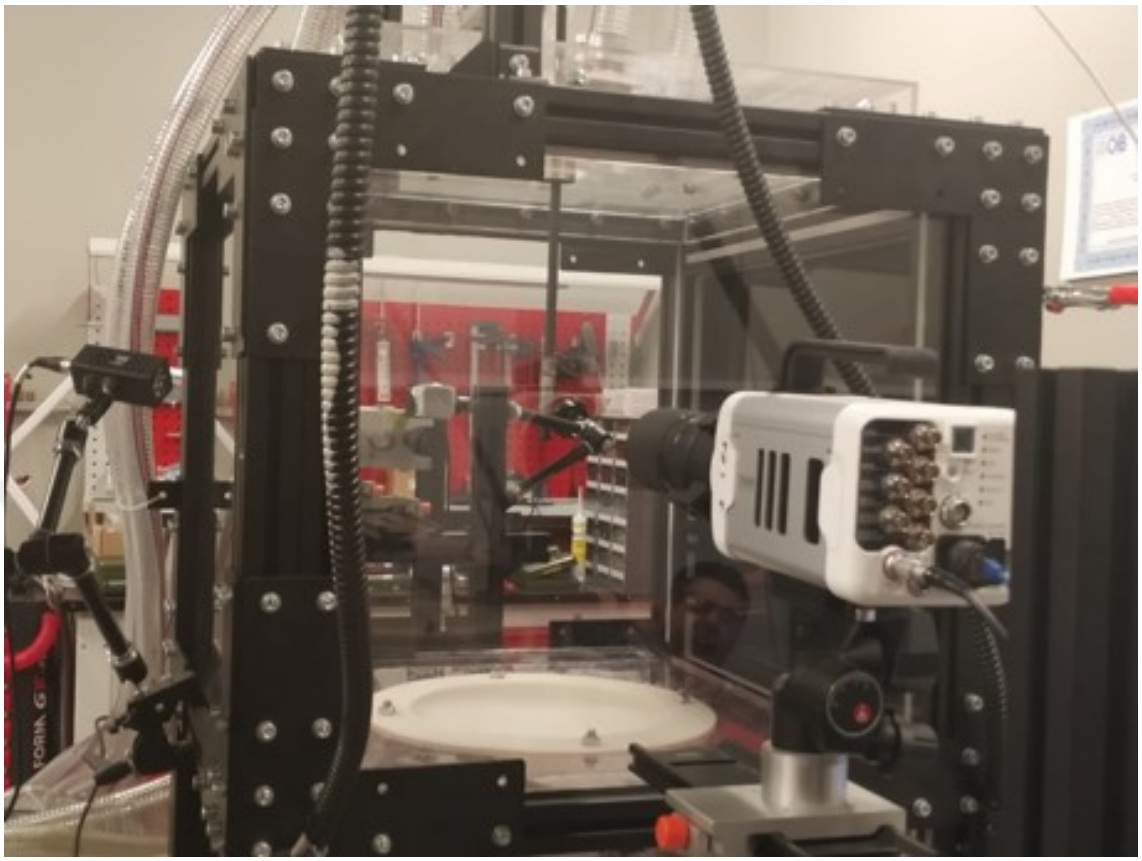

Figure 39: OzU Fluid Dynamics and Spray Laboratory test setup

The photos were taken with the Fastcam Mini UX50 camera, which can shoot up to 10,000 frame per second (FPS) at outlet of injector, opening, closing and spraying [46]. The images in the Figure 40 show photographs of the injector tip in the formation stages of the spray. The start and end of the spray must be clear for controlled atomization to occur. From the moment of stop, the injector must not allow any more liquid to escape from the atomizer.

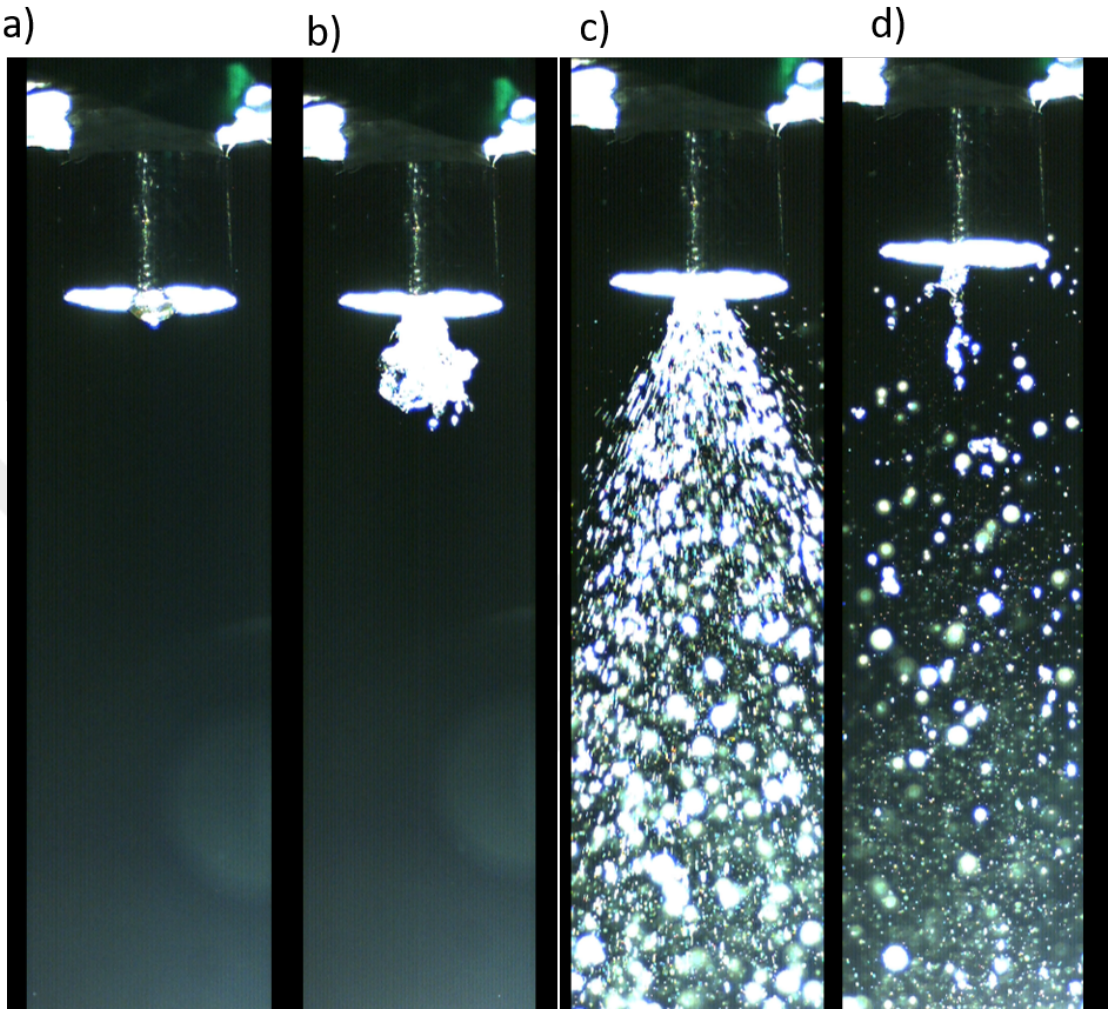

Figure 40: Spray steps **a)Closed:** Since no voltage is applied to the coil, the spring-loaded needle prevents the liquid from entering the atomizer.**b)Opening:** The movement of the needle is shown by the moment of the first flow. **c)Open:**By applying continuous voltage to the coil, the injector is kept open. **d)Closing:**As soon as the voltage is cut off, the spring force starts to dominate against other forces and closure occurs.

The performance of the atomizer is measured by these tests. Measured values include spray angle, droplet diameters, and liquid penetration.

6.2 Magneto-Static Analysis

Finite Element Methods (FEM) are used to solve electrical and magnetic field problems of solenoid actuators. The FEM can be derived using the basic principle of energy conservation [20]. Static electromagnetic field analysis of the solenoid actuator is done using ANSYS Electronic Suite. The electromagnetic force is calculated in ANSYS by Maxwell stress tensor as given below:

$$\vec{F}_{mag} = \iint \left\{ \frac{1}{\mu_0} \left(\vec{B}.\vec{n} \right) \vec{B} - \frac{1}{2\mu_0} \vec{B}^2.\vec{n} \right\} ds \tag{24}$$

where, n is a unit vector pointing out of surface.

Once the coil is energized, a magnetic field is generated. The magnetic flux forms a closed magnetic circuit through the plunger, solenoid case and solenoid magnetic circuit elements as shown in Fig 41. When the electromagnetic force is greater than the spring load force, the plunger and needle move toward solenoid, away from the seating position. When the coil is de-energized, the electromagnetic force disappears and the gap between seat and needle closes due to spring force. Therefore spring properties highly influence the design parameters such as the working pressures of the fluid acting on the needle.

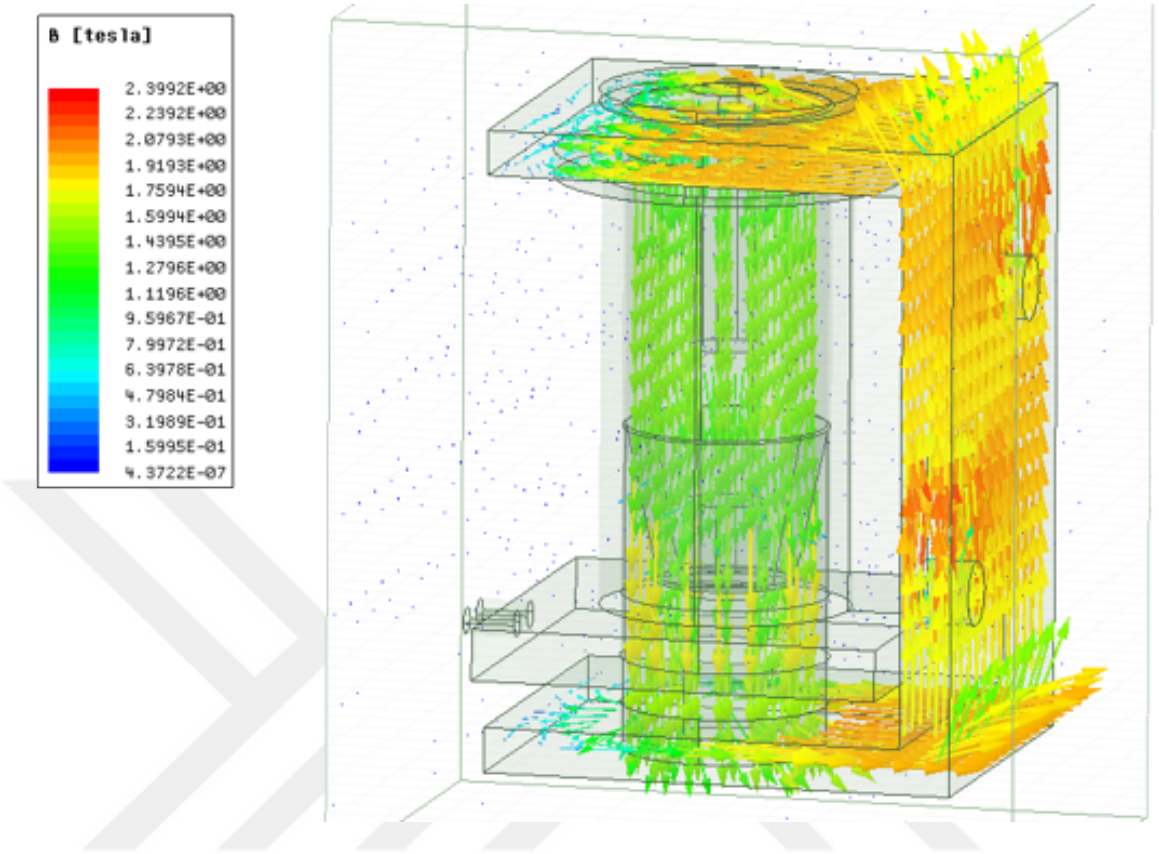

Figure 41: Magnetic flux vectors of injector solenoid is shown. The arrows indicate the direction of the magnetic flux. This flux forms a closed magnetic circuit.

Required magnetic force is verified using simulation with the spring parameters and fluid pressure as defined parameters. In this study, to find the electromagnetic force, magneto-statics analyses for 4 different air gaps and 3 different coil designs were performed. The properties of the used solenoids are given in Table 4. Results are given in Table 5.

Table 4: Properties of solenoids tested

Properties	**Model 1**	**Model 2**	**Model 3**
Wire diameter (mm)	0.2	0.25	0.25
Number of Turns	1000	675	530
Resistance (ohm)	24	12	8
Max current (24V)	1 A	2 A	3 A

Table 5: Simulation and experiment results of the solenoid actuator electromagnetic force [N]

Force [N]		Analysis			Experiment		
		Solenoid Current					
		1 A	2 A	3 A	1 A	2 A	3 A
Airgap	0 mm	13.41	18.50	22.78	13.45	18.80	22.40
	0.1 mm	10.76	15.19	18.34	11.10	15.48	18.30
	0.2 mm	9.31	13.55	16.41	9.50	13.39	16.20
	0.3 mm	8.26	13.04	14.68	8.40	12.80	14.90

To validate the results obtained from the simulations, an experimental setup was used to record the forces produced by different solenoid actuators at various opening and closing instances.

The experimental setup consisted of three different 24V DC operated solenoid actuators having the same physical properties, as were taken in the simulation phase. MATLAB Simulink software was interlinked with Quanser Q8 USB data acquisition

(DAQ) board to fetch the solenoid's push force from a load cell (FUTEK LSB-200) with resolution of 3.3 mN. The sensor readings are taken with 0.1 mm air gap increments (Fig 42 shows the test setup). Results of the experiment are given in Table 5.

The average error between simulation and experiments for the 1 A, 2 A, and 3 A solenoid actuators are, 0.178 N, 0.228 N, 0.213 N, respectively.

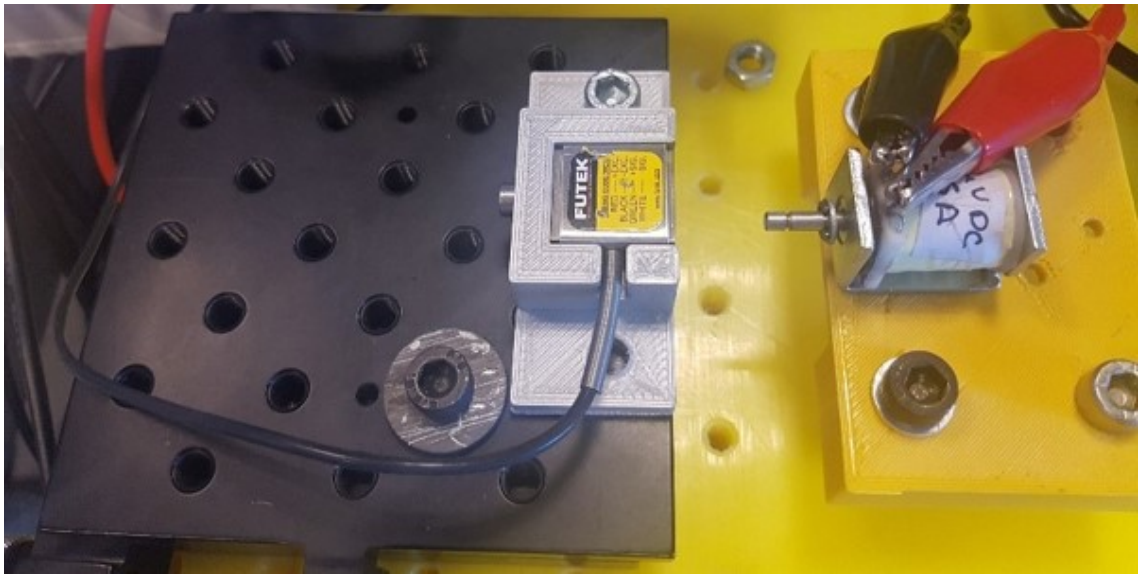

Figure 42: Test setup: Having a solenoid actuator fixed to a stationary support while the load cell being mounted on a linearly adjustable sliding surface to measure the force produced by the solenoid actuator

6.3 Spring Measurements System

The springs are the injector part used to eliminate the undesirable fluid flow of the injector. As a force against the force exerted by the fluid pressure on the needle, they ensure that the injector is closed when the coil is not energized. In addition, when the voltage applied to the coil is cut off, the current in the coil and the magnetic force on the plunger rapidly decrease. From this moment on, the spring force is responsible for closing the injector by placing the needle into the seat.

The main objective of the experiment was to find the force provided by various

springs at the different opening and closing instances. FUTEK Load cell was used to measure the force of different springs at a continuous increment of 0.1 mm from its most compressed position, which can be achieved by the test setup. The test setup is shown in Figure 43

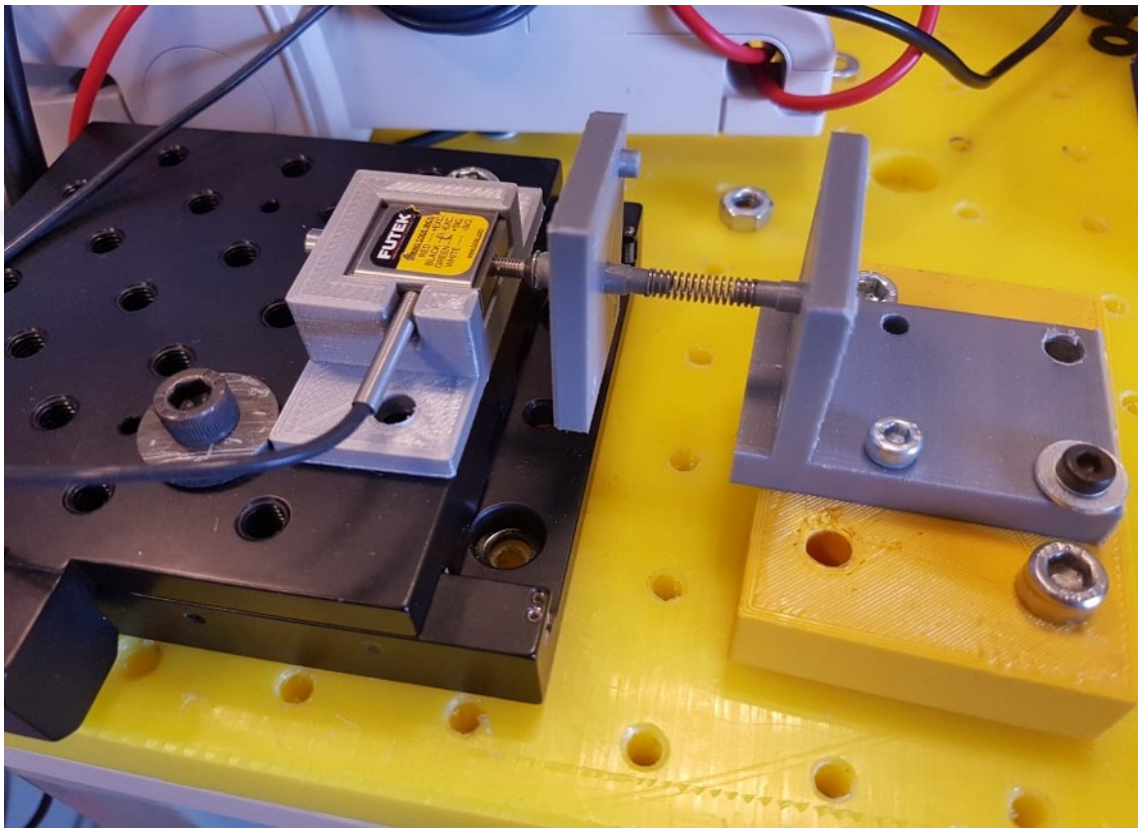

Figure 43: Spring test setup

MATLAB SIMULINK software inside the digital computer was used to get data from the Loadcell. USB data acquisition system (DAQ) which consisted of Quanser Q8 board was interlinked with MATLAB Simulink to get data from the Loadcell. All the above-stated process can be concluded by the block diagram representation in Figure 44.

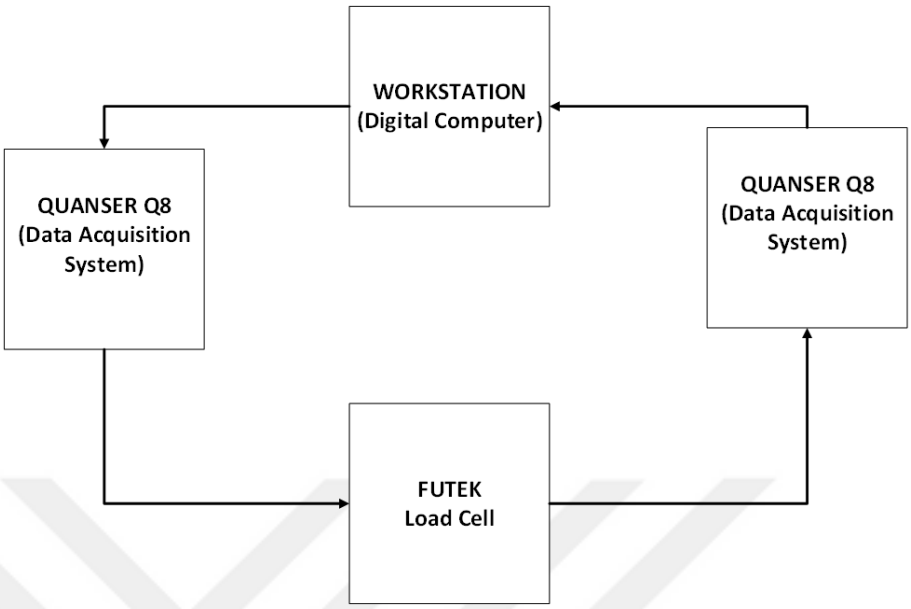

Figure 44: Block diagram of spring test overall process

Table 6: Spring Stiffness Coefficients

Test specimen	Spring Constant, 'K' [N/mm]
Spring 1	0.16559
Spring 2	0.088968
Spring 3	0.43423
Spring 4	0.1
Spring 5	0.10183
Spring 6	0.12973
Spring 7	0.13916
Spring 8	0.10956
Spring 9	0.27144

6.4 Transient Tests

It is very important to know the amount of liquid that the injector atomizes. One of the main tasks of the injector is to regulate the amount of liquid sprayed. Furthermore, the main task of the solenoid actuator is to control the fluid reaching the atomizer. For this purpose, the movement of the solenoid actuator plunger will open the throat of the injector channel and fluid goes to the atomizer. The characteristic of this movement will make it possible to know the amount of liquid to be sprayed from the injector.

Also, in some cases, a very small amount of liquid must be sprayed from the injector [47]. For this, the opening time was reduced to about 1 millisecond and the feasibility of such tests was demonstrated. A laser vibration measuring device was used for this test. The tank which gives liquid to the injector is pressurized up to 5 bar. The displacement was adjusted to about 80 microns. The starting and ending of the movement were recorded under these loads. The plunger of the solenoid actuator completed this distance in 1.2 milliseconds, as shown in the Figure 45

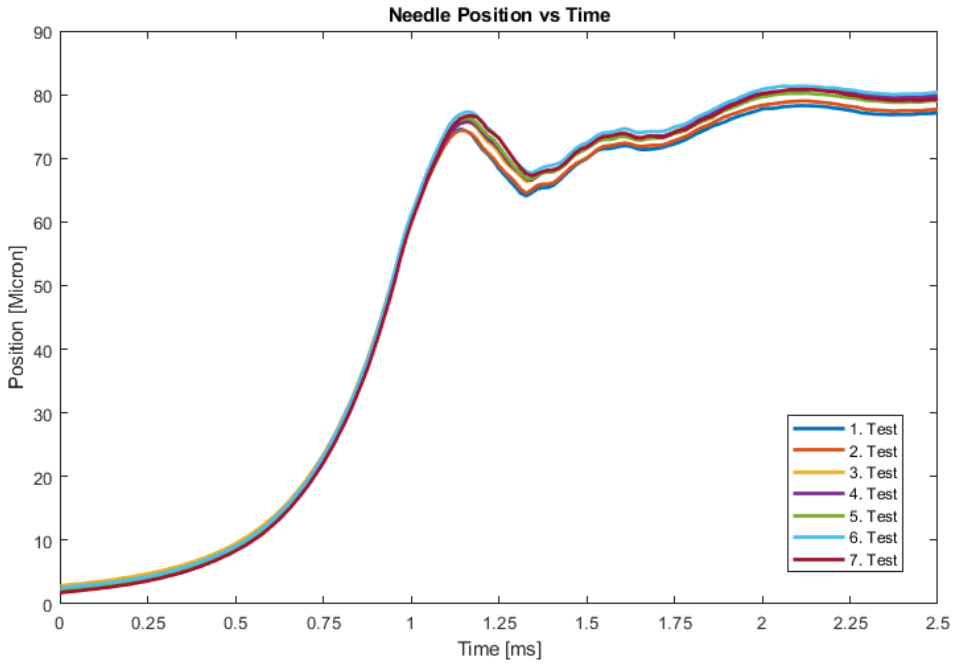

Figure 45: 2.2 Amper injector plunger position vs time test result under 5 bar fluid pressure. Position is meausred using the laser vibrometer. The duration of motion is 1.2 milliseconds and stroke 80 microns.

CHAPTER VII

CONCLUSION

Injectors are used to create spray and advanced types are used in the automotive industry. This study comprises the design of a solenoid based prototype injector with exchangeable core elements for research and development purposes. The developed injector will be used in the automotive industry for spraying urea to clean exhaust gases.

First, the operating principles of a solenoid actuator and effect of used material to the dynamic behavior were explained. Solenoid actuators were modeled and then electrical, magnetic and mechanical subsystems were defined. The coupling between these subsystems was examined.

In literature injectors are categorized into two types, and each of these is explained, and our design examples were presented. Physical models were described for each injector mechanism. Variables in these models that can regulate the injector's performance were explained. The pool-type injector was decided to be more suitable for its modularity.

Also, pool type injector design was finalized and then manufactured. Due to fluid leakage from the tip of the first design, a new one was made. The leakage problem in the dynamic motion zone was examined in detail and surface roughness and gasket types were studied to ensure proper sealing. The manufacturing methods for the injector needle were explained in detail. The final design is leak-proof and worked successfully in the tests.

The test and analysis stage of the solenoid based prototype injector has been

reached. The electro-magneto-mechanical component of the injector system was focused and the electromagnetic simulations of the solenoid actuator were verified with experiments. The solenoid based prototype injector was tested under strict circumstances comparable to commercial injectors and opened in 1.2 milliseconds at about 80 micrometers stroke under 5 bar fluid pressure effectively.

The results show that the prototype injector's finite element based simulations work accurately, and reliable results can be achieved with changeable injector parts. Furthermore, as the prototype model allows easy changing of the core elements, the researchers could benefit from the design and development processes offered here greatly.

APPENDIX A

CAD, MANUFACTURED AND CROSS-SECTION OF PROTOTYPE INJECTOR

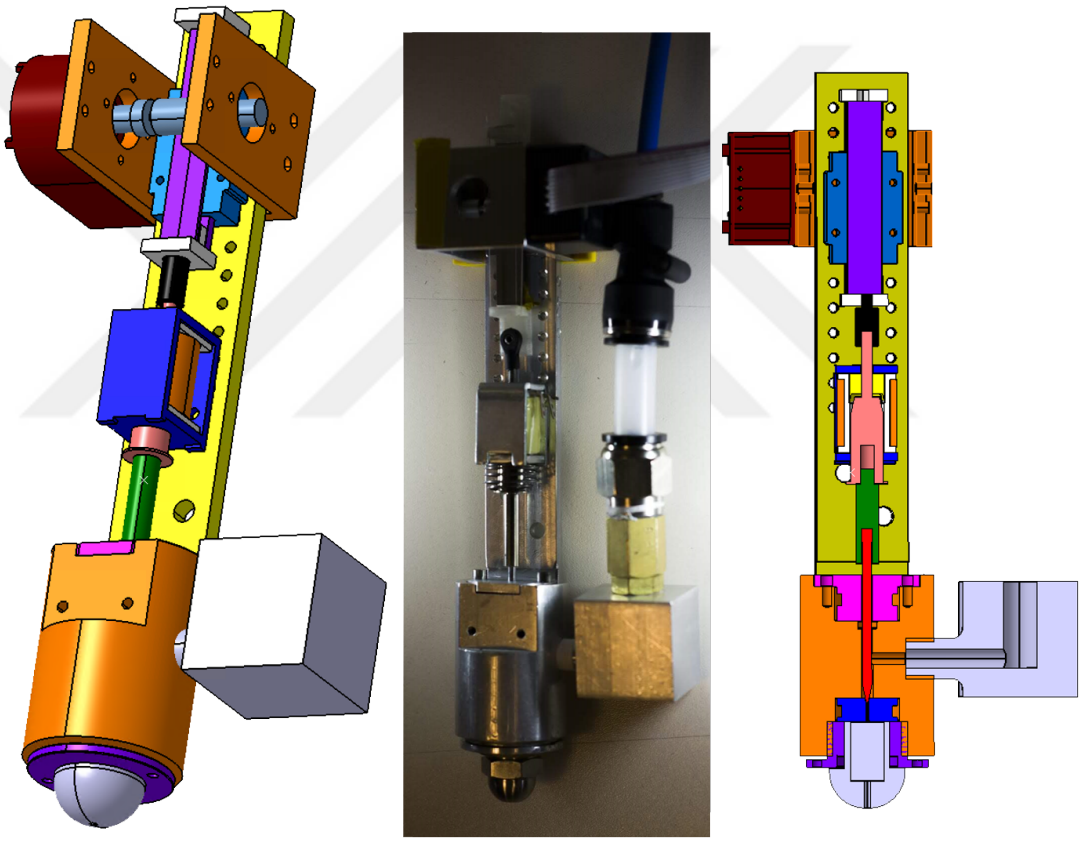

APPENDIX B

PARAMETRIC ANALYSIS FLUX DENSITY RESULTS

Cross section view of solenoid actuator and magnetic flux density of 50JN1000 steel solenoid are shown over time. Respectively, starting the motion, in the middle of the movement, at the end of the movement and in 30 milliseconds

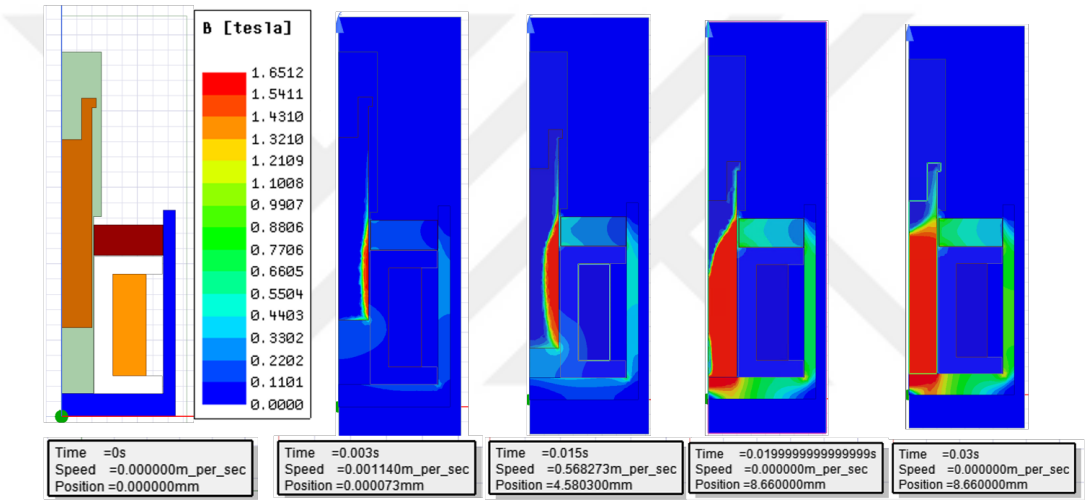

Cross section view of solenoid actuator and magnetic flux density of Supercore 10JNEX900 steel solenoid are shown over time. Respectively, starting the motion, in the middle of the movement, at the end of the movement and in 30 milliseconds

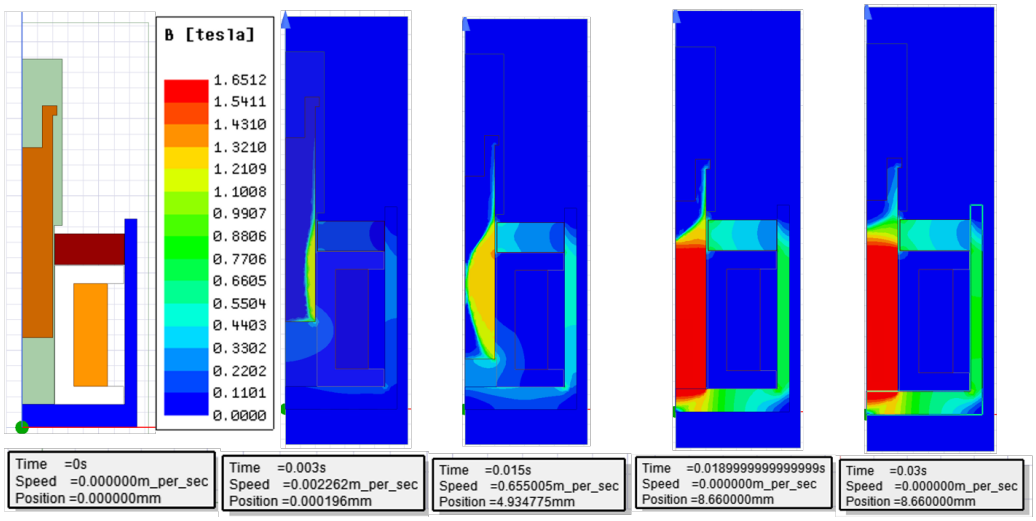

Cross section view of solenoid actuator and magnetic flux density of 50JNA350 steel solenoid are shown over time. Respectively, starting the motion, in the middle of the movement, at the end of the movement and in 30 milliseconds

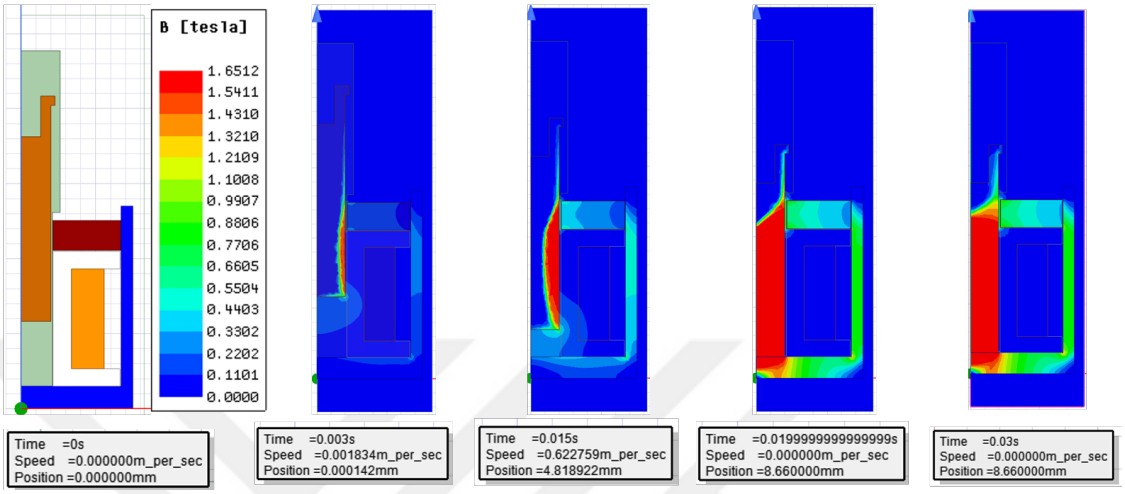

Bibliography

[1] Rotex Automation Limited, "Solenoid valve, automotive solenoid valve - rotex automation," 2019.

[2] German Association of the Automotive Industry, "AdBlue®," tech. rep., Verband der Automonilindustrie, 2013.

[3] Q. Cheng, Z. Zhang, and N. Xie, "Power losses and dynamic response analysis of ultra-high speed solenoid injector within different driven strategies," *Applied Thermal Engineering*, vol. 91, pp. 611 – 621, 2015.

[4] A. Yagcı, M. Kuntuz, and O. Bebek, "Electromagnetic and dynamic analysis of solenoid actuator to reduce the closing time," in *9th ANKARA INTERNATIONAL AEROSPACE CONFERENCE*, September 2017.

[5] A. Yagcı, S. Qureshi, M. Kuntuz, and O. Bebek, "Design of a solenoid based prototype injector for evaluation of electromagnetic parameters," in *19th International Symposium on Electromagnetic Fields in Mechatronics, Electrical and Electronic Engineering*, 2019.

[6] S. Li, T. W. Nehl, S. Gopalakrishnan, A. M. Omekanda, C. Namuduri, and R. Prasad, "A dynamic solenoid model for fuel injectors," *2018 IEEE Energy Conversion Congress and Exposition (ECCE)*, pp. 3206–3213, 2018.

[7] X. Yao, Z. Zhang, X. Kong, and C. Yin, "Dynamic response analysis and structure optimization of gdi injector based on mathematical model," *International Journal of Reliability, Quality and Safety Engineering*, vol. 25, 12 2017.

[8] X. Kong and S. Li, "Dynamic performance of high speed solenoid valve with parallel coils," *Chinese Journal of Mechanical Engineering*, vol. 27, pp. 816–821, 07 2014.

[9] S. Al-Saqer and G. M. Hassan, "Optimization of solenoid valve for variable rate application system," *American Journal of Agricultural and Biological Science*, vol. 6, pp. 348–355, 08 2011.

[10] S. Angadi, R. Jackson, S.-Y. Choe, G. Flowers, J. Suhling, Y.-K. Chang, and J.-K. Ham, "Reliability and life study of hydraulic solenoid valve. part 1: A multi-physics finite element model," *Engineering Failure Analysis*, vol. 16, no. 3, pp. 874 – 887, 2009.

[11] B. Lequesne, "Fast-acting, long-stroke solenoids with two springs," in *Conference Record of the IEEE Industry Applications Society Annual Meeting,*, pp. 195–202 vol.1, Oct 1989.

[12] M. Kabib, M. L. Batan, B. Pramujati, and A. S. I. Sigit, "Modelling and simulation analysis of solenoid valve for spring constant influence to dynamic response," *ARPN Journal of Engineering and Applied Sciences*, vol. 11, pp. 2790–2793 vol.11, 02 2016.

[13] A. Subic and D. Cvetkovic, "Virtual design and development of compact fast-acting fuel injector solenoid actuator," *International Journal of Vehicle Design*, vol. 46, 06 2008.

[14] B. Cai, Y. Liu, X. Tian, Z. Wang, F. Wang, H. Li, and R. Ji, "Optimization of submersible solenoid valves for subsea blowout preventers," *Magnetics, IEEE Transactions on*, vol. 47, pp. 451 – 458, 03 2011.

[15] S. Baek, H. Kim, D. Jang, S. Lee, Y. Kwon, E. Ro, and C. Lee, "Structural optimization for nonlinear dynamic response of solenoid actuator," *Transactions of the Korean Society of Automotive Engineers*, vol. 21, 01 2013.

[16] D. Cvetkovic, I. Cosic, and A. Subic, "Improved performance of the electromagnetic fuel injector solenoid actuator using a modelling approach," *International Journal of Applied Electromagnetics and Mechanics*, vol. 27, pp. 251–273, 04 2008.

[17] B. Lequesne, "Fast-acting long-stroke bistable solenoids with moving permanent magnets," *IEEE Transactions on Industry Applications*, vol. 26, pp. 401–407, May 1990.

[18] F. Bayat, A. Fadaie Tehrani, and M. Danesh, "Finite element analysis of proportional solenoid characteristics in hydraulic valves," *International Journal of Automotive Technology*, vol. 13, pp. 809–816, Aug 2012.

[19] ANSYS, Inc, "Electromagnetic suite," 2017.

[20] J. Brauer, *Magnetic Actuators and Sensors*. Wiley, 2014.

[21] J. M. D. Coey, *Magnetism and Magnetic Materials*. Cambridge University Press, 2010.

[22] Q. Cheng, Z. Zhang, and N. Xie, "Multi-physical fields coupling simulation and performances analysis of a novel heated-tip injector," *Journal of Thermophysics and Heat Transfer*, vol. 30, pp. 1–12, 04 2016.

[23] S.-I. Lee and S.-Y. Park, "Numerical analysis of internal flow characteristics of urea injectors for scr dosing system," *Fuel*, vol. 129, pp. 54 – 60, 2014.

[24] O. E. Nural and Özgür Ertunç, "Predicting the performance of pressure-swirl atomizers," *Atomization and Sprays*, vol. 28, no. 6, pp. 481–546, 2018.

[25] E.-J. Gwak and S.-Y. Park, "Study on the flow characteristics of urea-scr swirl injector according to the needle lift profile," *Journal of the Korea Academia-Industrial cooperation Society*, vol. 17, pp. 650–655, 01 2016.

[26] Y. Kim and S. Cho, "New technologies for the super clean passenger car diesel engines," *Auto Journal, KSAE*, vol. 31, no. 5, pp. 16–24, 2009.

[27] I. S. Jo, M. C. Chung, S. M. Kim, G. S. Sung, and J. W. Lee, "Experimental investigation and hydraulic simulation of dynamic effects on diesel injection characteristics in indirect acting piezo-driven injector with bypass-circuit system," *International Journal of Automotive Technology*, vol. 16, pp. 173–182, Apr 2015.

[28] d'Ambrosio S. and F. A., "Diesel engines equipped with piezoelectric and solenoid injectors: hydraulic performance of the injectors and comparison of the emissions, noise and fuel consumption," *Applied Energy*, vol. 211, pp. 1324 – 1342, 2018.

[29] Y. W. H. Guo and Q. Wen, "Investigation on comprehensive performance of the efi by mim technology," *Journal of Applied Electromagnetics and Mechanics*, vol. 42, pp. 579–588, 2013.

[30] Q. Xiong, Y. Zhang, and J. Wang, "Development of a high-speed solenoid valve measuring bench," in *2009 International Conference on Information Technology and Computer Science*, vol. 2, pp. 421–424, July 2009.

[31] N. B. Hung, O. Lim, and S. Yoon, "Effects of structural parameters on operating characteristics of a solenoid injector," *Energy Procedia*, vol. 105, pp. 1771 – 1775, 2017. 8th International Conference on Applied Energy, ICAE2016, 8-11 October 2016, Beijing, China.

[32] S.-I. Lee and S.-Y. Park, "Numerical analysis of internal flow characteristics of urea injectors for scr dosing system," *Fuel*, vol. 129, pp. 54 – 60, 2014.

[33] H. Hong and B. Torab, "Solenoid-operated diesel injectors for low-viscosity liquid and gaseous fuels," *Proceedings of The Institution of Mechanical Engineers Part D-journal of Automobile Engineering - PROC INST MECH ENG D-J AUTO*, vol. 215, pp. 1281–1296, 01 2001.

[34] H. Chowdhury, S. Mazlan, and A. G. Olabi, "A simulation study of magnetostrictive material terfenol-d in automotive cng fuel injection actuation," *Solid State Phenomena*, vol. 154, pp. 41–46, 04 2009.

[35] A. Pawlak, *Sensors and actuators in mechatronics: Design and applications*. 01 2017.

[36] Agient Technologies, *Agilent 1146B AC/DC Current Probe - User's Guide*. Agient Technologies, 2013.

[37] Z. Jingqiu and O. Guangyao, "Optimization design of the electronically controlled injector," in *International Conference on Mechatronics and Automation*, pp. 1996 – 2001, 09 2009.

[38] P. Oxley, J. Goodell, and R. Molt, "Magnetic properties of stainless steels at room and cryogenic temperatures," *Journal of Magnetism and Magnetic Materials - J MAGN MAGN MATER*, vol. 321, pp. 2107–2114, 07 2009.

[39] S. Marčič, M. Marcic, and Z. Praunseis, "Mathematical model for the injector of a common rail fuel-injection system," *Engineering*, vol. 07, pp. 307–321, 01 2015.

[40] Y. Çengel and A. Ghajar, *Heat and Mass Transfer: Fundamentals & Applications*. McGraw-Hill, 2010.

[41] X. Seykens, L. Somers, and R. Baert, "Modeling of common rail fuel injection system and influence of fluid properties on injection process," 01 2004.

[42] L. Landau and E. Lifshitz, *Fluid Mechanics*. No. 6. c., Elsevier Science, 2013.

[43] KASTAŞ Sealing Technologies Inc., *Hydraulic Piston-Throat Seals*, 2018.

[44] ANCA Inc., "Anca mx7 linear," 10 2019.

[45] M. Polat Kuntuz, S. Qureshi, and O. Bebek, "Sliding mode control of an electromechanical solenoid actuator for soft landing," pp. 369–374, 08 2018.

[46] Photron, *FASTCAM Mini UX50/100 Hardware Manual*. Photron Limited.

[47] L. Passarini and M. Pinotti, "A new model for fast-acting electromagnetic fuel injector analysis and design," *Journal of the Brazilian Society of Mechanical Sciences and Engineering*, vol. 25, 03 2003.

[48] Z. Kamis, *Electromechanical actuators desgn for valves and researching*. PhD thesis, Uludag University.

[49] Z. Kamış and I. Yüksel, "The investigation of the design parameters of electromagnetic valve actuation systems," *Uludağ University Journal of The Faculty of Engineering*, vol. 9, 08 2004.

[50] B. P. Lequesne, "Finite-element analysis of a constant-force solenoid for fluid flow control," *IEEE Transactions on Industry Applications*, vol. 24, pp. 574–581, July 1988.

[51] E. Plavec and M. Vidović, "Genetic algorithm based plunger shape optimization of dc solenoid electromagnetic actuator," in *2016 24th Telecommunications Forum (TELFOR)*, pp. 1–4, Nov 2016.

[52] Q. Cheng, M. Xu, Z. Zhang, and N. Xie, "Investigation on the spray characteristics of standard gasoline, n-pentane, iso-octane and ethnaol with a novel heated tip sidi injector," *Applied Thermal Engineering*, vol. 110, 08 2016.

[53] L. Wang, G.-X. Li, C.-L. Xu, X. Xi, X.-J. Wu, and S.-P. Sun, "Effect of characteristic parameters on the magnetic properties of solenoid valve for high-pressure common rail diesel engine," *Energy Conversion and Management*, vol. 127, pp. 656 – 666, 2016.

[54] N. Balasubramanian, T. Iwaszkiewicz, and J. Sethuraman, "High speed visualization of gasoline pump injector (gpi)," in *28th Conference on Liquid Atomization and Spray Systems*, (Valencia, Spain), 6-8 September 2017.

VITA

Ayhan Yağcı was born in 1991 in Eskişehir. He received the B.Sc. degree in Astronautical Engineering Department from Istanbul Technical University, Istanbul, Turkey, 2015. He was the founder and leader of ITU PARS Rocket Group between March 2012 to September 2014. After receiving his B.Sc. degree, he started his master studies at Özyeğin University Mechanical Engineering Department. He worked as a research assistant at Özyeğin University Robotic Laboratory, under the supervision of Asst. Prof. Özkan Bebek. In May 2019, he established Dipol Technology and Engineering which is a solenoid actuator and solenoid valve design, analysis, testing, and manufacturing company. His research interests include electromagnetic actuators, system design, and FEM analysis.